Influences of SiO_2 and Fe_2O_3 on penetration of low carbon steel during GTA-welding

Master thesis

June 1999

J.E. Janse

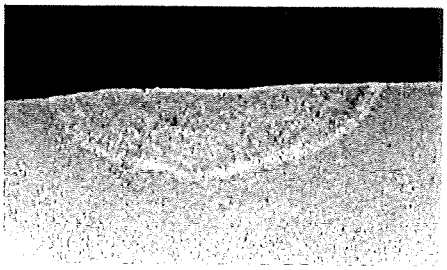

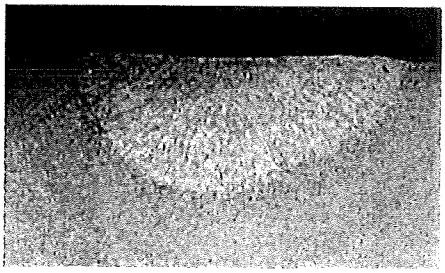

TU Delft
Delft University of Technology

Faculty of Applied Sciences
Laboratory of Materials Science and Engineering
Section Welding Technology and Non-Destructive Testing

M. Hermans

Summary

In the section Welding Technology and Non-Destructive Testing of the Department of Materials Science and Engineering research is carried out with the aim to develop a new position sensing system. Additives that influence the arc voltage are hereby used as tracer. By marking the seam before welding with an additive, it is possible to control the position of the torch by monitoring the arc voltage and correcting for deviations. SiO_2 and Fe_2O_3 have proven to meet the required properties and can be used as additive.

In this research project the effects of SiO_2 and Fe_2O_3 on the formation of the weld pool were studied. Bead-on-plate experiments show considerable changes in arc behaviour and weld pool dimensions when additives were applied on the surface. Also differences between SiO_2 and Fe_2O_3 are noticed. The experimental results are thought to be caused by three mechanisms: arc constriction, arc root deformation and Marangoni flow. Arc root deformation seems to play a more important role in the case of welding with SiO_2 than in the case of welding with Fe_2O_3. This emphasises the importance of the properties of the additive that is applied on the surface.

Chemical analyses of the weld show that the oxygen concentration of the weld pool alters but more accurate analyses should be performed. A decrease in Mn concentration give the impression that manganese silicates are formed when SiO_2 is used as additive. Vickers hardness measurements were carried out and show only a slight difference in hardness of the weld. Photographs of the structure of the weld supports the results of the hardness measurements.

Furthermore, the surface tension of molten metal in the weld pool was examined by measuring the oscillation frequency of the weld pool at different temperatures for welds with and without SiO_2. Considerable differences between the surface tension of both types of welds were found. However, the surface tension temperature coefficient was found to be negative for both welds, which is probably caused by the high temperature of the weld pool. Improvement of this measurement technique is recommended.

Samenvatting

Binnen de sectie Lastechnologie en NDO wordt onderzoek gedaan naar een nieuw plaatsbepalings-systeem voor de GTA-lasboog, waarbij gebruik gemaakt wordt van additieven. Voor het lassen wordt de lasnaad gemarkeerd met een oxidepasta die de boogspanning beïnvloedt. Zo is het mogelijk om tijdens het lassen de plaats van de boog te bepalen en de boog bij te sturen. SiO_2 and Fe_2O_3 hebben voldoende invloed op de boogspanning om als additief gebruikt te kunnen worden.

Bij dit project zijn de invloeden van SiO_2 and Fe_2O_3 op de vorming van het lasbad onderzocht. Experimenten tonen duidelijke veranderingen in booggedrag en lasbadvorm wanneer er over additieven gelast wordt. Ook verschillen tussen invloeden van SiO_2 and Fe_2O_3 op de vorm van het lasbad zijn waargenomen. Drie mechanismes zouden de experimentele resultaten kunnen verklaren: boogcontractie, verandering in boog-plaatcontact en Marangoni stromingen. Bij SiO_2 blijkt vooral de vervorming van het boog-plaatcontact een grote invloed te hebben op de vorming van het lasbad. Bij Fe_2O_3 speelt dit een veel minder belangrijke rol. Onder andere hieruit blijkt dat de fysische eigenschappen van het additief belangrijk zijn voor de invloed die het additief op de lasbadvorming zal hebben.

Chemische analyse van het lasmetaal laten een verandering in zuurstofgehalte zien, maar een uitgebreidere analyse is hier gewenst. Veranderingen in de Mn concentratie doen vermoeden dat Mn met Si verbindingen vormt wanneer SiO_2 als additief is gebruikt. Vickers hardheidsmetingen tonen een kleine afname in hardheid wanneer SiO_2 of Fe_2O_3 zijn gebruikt. Dit kan veroorzaakt zijn door een verandering in de warmteïnbreng, wat ondersteund wordt door structuuronderzoek.

De oppervlaktespanning van het gesmolten metaal in het lasbad is onderzocht door het bepalen van de oscillatiefrequentie van het lasbad bij verschillende temperaturen. Dit is uitgevoerd voor lassen met en zonder SiO_2. Duidelijke verschillen in oppervlaktespanning zijn gevonden. In beide gevallen neemt de oppervlaktespanning af met toenemende temperatuur. Dit laatste is waarschijnlijk het gevolg van de hoge temperatuur in het lasbad waarbij oppervlakte-actieve stoffen niet meer actief zijn.

Contents

1. Introduction

Gas Tungsten Arc welding (GTA-welding) is a widely used fusion technique in welding industry. This process is particularly suited for welding with considerable precision and a high level of quality. Over the last years sensors and robots are developed to automate this welding process. In the section Welding Technology and Non-Destructive-Testing of the Department of Materials Science and Engineering research is carried out with the aim to develop a new position sensing system. Additives that influence the arc voltage are hereby used as tracer. By marking the seam before welding with such an additive, it is possible to control the position of the torch by monitoring the arc voltage and correcting for deviations.

In previous research [1] various additives were extensively tested on their suitability as tracer. Most important criterion is that the additive has a sufficiently large effect on the arc voltage of the welding arc. Especially oxides, like SiO_2 and Fe_2O_3, have proven to produce the required effect.

This research project is concentrated on influences that additives have on weld pool characteristics. Bead-on-plate experiments were carried out on low carbon steel, Fe360, with SiO_2 or Fe_2O_3 as additives applied on the surface. Welding current, travel speed and arc length were varied in order to obtain more insight in the mechanisms that cause variations in weld pool characteristics. The weld pool shape was examined by measuring depth, width and area of transverse cross-sections. Additionally, by blowing molten metal out of weld pools also the length of the weld pool could be determined. Chemical analysis and Vickers hardness measurements were carried out and photographs were taken to analyse the structure of the weld (weld metal, HAZ and base material). Furthermore, the surface tension temperature coefficient of molten metal in the weld pool was examined by measuring the natural oscillation frequency of the weld pool at different temperatures for blank steel and steel with SiO_2 added.

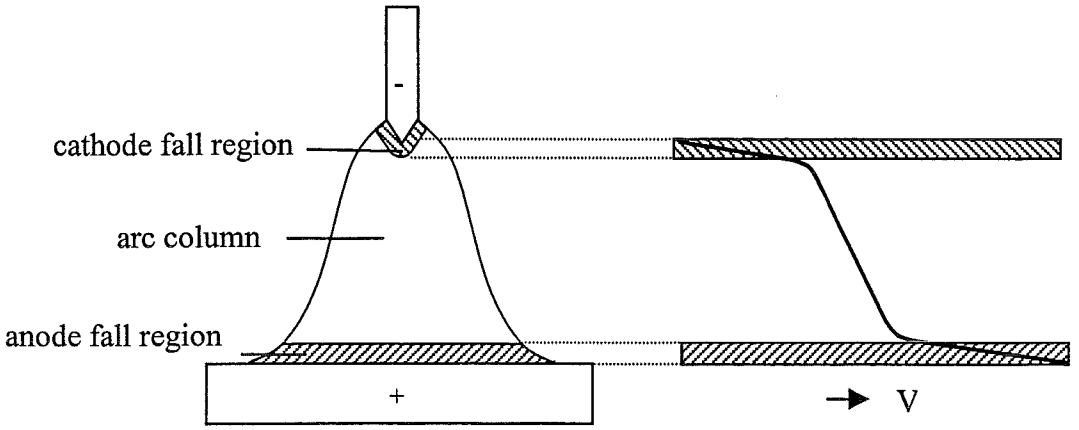

Fig. 2.1. Welding arc with non-linear voltage path.

2. GTA-welding

2.1 General introduction

Gas Tungsten Arc welding (GTA-welding) belongs together with Metal Inert Arc welding (GMA-welding) to the group of electric arc welding process. These welding processes can be characterised by the presence of a stable arc between electrode and workpiece. In GTA-welding non-melting tungsten electrodes are used, enriched with a low percentage of thorium- or zirconium oxide. Furthermore, a shielding gas, like argon or helium is applied to protect electrode and weld pool from the surrounding atmosphere.

In this chapter properties of the welding arc and weld pool for GTA-welding are presented. Forces acting on the weld pool are summarised as well as influences of additives on weld pool characteristics. Finally, the most important features of surface tension in the weld pool are presented in more detail.

2.2 Welding arc

The welding arc can be described as a stable discharge in the present gas or vapour. It contains electrons, ions and gas molecules originating from weld metal, shielding gas or electrode. Roughly three regions can be distinguished in the arc: anode fall region, arc column and cathode fall region, as shown in Fig. 2.1.

In the arc electrical energy is developed, which under stationary circumstances dissipates in the form of heat conduction, convection and radiation. The electrical energy generated per time unit, E, can be written as:

$$E = V \times I \tag{2.1}$$

in which V and I are the total arc voltage [V] and the welding current [A]. It is shown in Fig. 2.1 that large voltage drops are present in the anode and cathode fall region. Consequently most of the energy is developed near the electrode and the workpiece [2].

2.2.1 Heat generated in the welding arc

Heat transport from the arc to the workpiece is important for the welding process and has been the subject of many investigations [3-9]. Heat input to the workpiece, here the anode, is a result of the voltage drop in the anode fall region, the thermal energy of the electrons, the work function of the base material and the contribution from the arc column. This is expressed in the following equation:

$$Q_a = V_a I + 3\frac{k\Delta T}{2e} I + \frac{\phi_a}{e} I + c_a V_p I \qquad (2.2)$$

in which Q_a represents the heat input to the anode [J/s], V_a the voltage drop over the anode fall region [V], I the welding current [A], k the Boltzmann constant [J/K], ΔT the temperature difference between the arc column and the anode [K], e the elementary electric charge and ϕ_a the work function of the anode [eV]. The constant, c_a, in the last term indicates that only part of the heat generated in the arc column is transferred to the workpiece. Plasma convection forms the most important contribution for this heat transfer. Electromagnetic forces in the arc column, also called Lorentz-forces mainly induce plasma convection in the arc. By interaction of the welding current, arc magnetic field and charge carriers in the arc a pressure is built up in the centre of the arc. The pressure increases when the radius of the arc becomes smaller or the welding current increases [3].

2.2.2 Efficiency of the welding process

Process efficiency and melting efficiency express the amount of heat that is transferred to the workpiece or used for melting. The process efficiency η_p is defined as the percentage of the total energy generated in the arc that is transported to the workpiece:

$$\eta_p = \frac{Q}{V_t I} \times 100\% \qquad (2.3)$$

in which Q represents the energy transferred to the workpiece [J/s] and V_t and I are the total arc voltage and welding current respectively. GTA welding has a process efficiency of 50-80% [2,3,9].

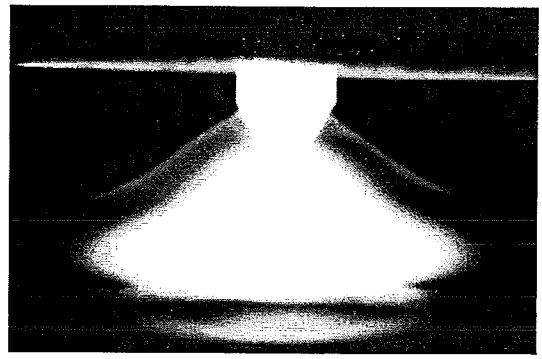

a

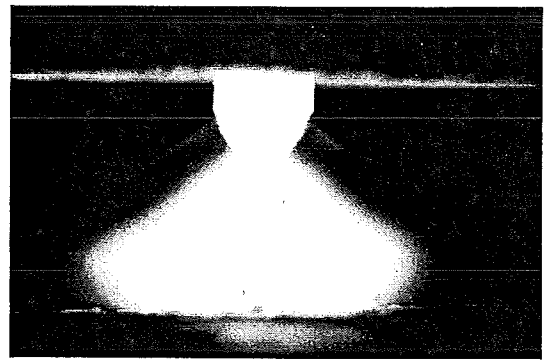

b

Fig. 2.2. Front view of GTA-welding arc [1]:
a. blank steel
b. with SiO_2

The efficiency of the welding process can also be expressed in terms of the melting efficiency, η_m. The melting efficiency is defined as the fraction of the transported energy used for heating from room temperature and melting the base material:

$$\eta_m = \frac{q\,A\,v}{V\,I} \tag{2.4}$$

in which q represents the heat required to heat and melt a unit volume of metal [J/m^3], A is the transverse cross-sectional area [m^2] and v the travel speed [m/s]. GTA-welding has a melting efficiency of 20-40% [2]. It appears that the melting efficiency is a function of the energy density. Higher energy density causes a faster heating of the metal and therefore less heat can dissipate through heat conduction in the workpiece [10].

2.2.3 Influences of additives

Additives may have an enormous influence on the welding arc properties. Constriction of the arc and arc trailing are two phenomena induced by the presence of a layer of additives at the surface of the workpiece.

Constriction of the arc

During welding with certain additives constriction of the welding arc occurs, as shown in Fig. 2.2. Several researchers came to the conclusion that constriction of the arc is caused by the presence of vaporised additive in the outer region of the arc [1,11,12]. The temperature in the centre of the arc is so high that gas and additive atoms are ionised to electrons and positive ions. However, in the cooler outer regions of the arc the vapour exists as molecules and dissociated atoms, which are large enough to capture electrons and form negative ions. Consequently, the number of electrons is reduced thereby increasing the voltage drop and forcing the arc to constrict.

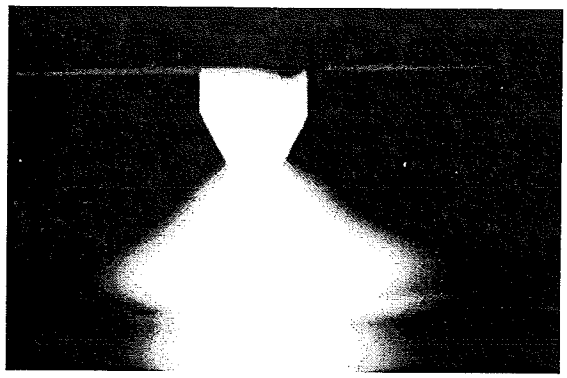

a

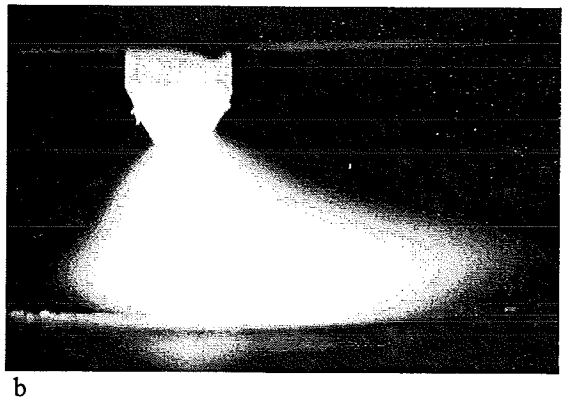

b

Fig. 2.3. Side view of GTA-welding arc [1]:
a. blank steel
b. with SiO_2

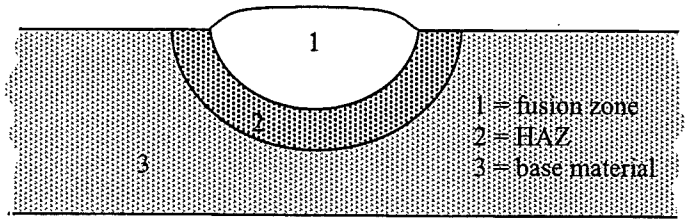

Fig. 2.4. Schematic representation of a weld.

The amount of additive present and the effectiveness of the additive to combine with electrons determine the degree of arc constriction. While additives also dissipate away from the arc a constant flow of new additive is necessary to ensure the constricting effect. This was confirmed by stationary welding tests [13], where after 10 seconds arc constriction was found to diminish (using a current of 50 A on stainless steel).

For welding with high welding current (>250 A) the degree of arc constriction becomes considerably smaller. This also can be explained with a lower concentration of vaporised additive in the arc. Higher welding currents cause an increase in Lorentz forces in the arc and induce a larger gas vortex. This supports a faster removal of the additive preventing the arc to constrict [14].

Arc trailing

Besides arc constriction a second effect, called arc trailing, occurs when an additive is applied on the workpiece. As the arc reaches the oxide layer it remains behind with respect to the electrode resulting in a longer effective arc length [1]. This effect is clearly shown on photographs of the arc taken perpendicular to the welding direction, Fig. 2.3. The photographs were taken at a travel speed of 4 mm/s. Elongation of the effective arc length causes an increase in arc voltage when the welding current is kept constant.

2.3 Weld pool

Heating and melting of metals have great impact on their structure and mechanical properties. Therefore it is important that welding is performed under optimal welding conditions. Research to the mechanism of weld pool formation, weld structure and mechanical properties of the weld has been performed in order to obtain more knowledge about welding process.

The weld pool is that part of the workpiece that is melted during the welding process. In solidified state it often is referred to as fusion zone. The part of the workpiece where the structure is influenced by temperature changes but no melting occurs, is called the heat-affected zone (HAZ). Both are shown in Fig. 2.4.

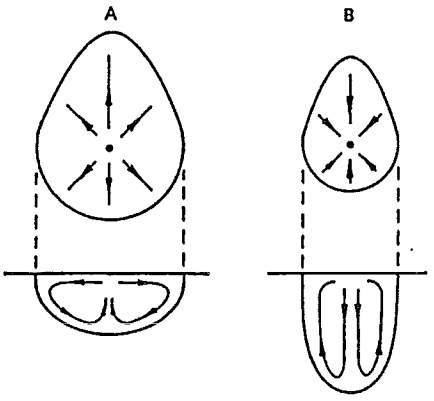

Fig. 2.5. Schematic representation of two possible flows in the weld pool.

Dimensions of the weld pool and heat-affected zone are important in the welding industry while they affect the quality of the joint. The depth must be large enough to obtain full penetration, but not to large that undercutting occurs. The width of the weld pool is preferred to be as small as possible in order to minimise the amount of affected workpiece. One way to express the shape of the weld pool is the so-called depth-to-width (D/W) ratio, which is an indication for the penetration properties of the weld.

Several computer models have been developed predict the weld pool dimensions under different welding conditions [15-17]. These models consider the weld pool formation to be governed by the flow pattern in the liquid metal. This pattern is induced by several forces: Lorentz force, Marangoni force, drag force and buoyancy force. They are controlled by welding parameters as current, travel speed and arc length. An overview of the forces of the weld pool and the effects of welding parameters are given in the next sections. Additionally, influences of additives on the weld pool as found in literature are presented.

2.3.1 Forces in the weld pool

Weld penetration is a function of heat transport in the weld pool. Heat transport in the weld pool is strongly affected by the fluid flow pattern [18, 19]. Four forces influence the fluid flow pattern in the weld pool [20, 21]: the Lorentz force, the Marangoni force, the drag force and the buoyancy force.

Lorentz force

The electric current flows from the electrode to the workpiece and disperses in the weld pool. When a current flows through a fluid conductor a magnetic field sets up around it, producing a self-compressive force on the conductor, the Lorentz force. In a situation where the welding current disperses this leads to pressure build-up, with the largest increase in pressure there where the current density is the highest. The formed pressure gradient leads to a flow of conducting fluid from regions of high current to regions of low current. This results in a flow from the centre of the weld pool towards the edge, as a flow of type B, Fig. 2.5.

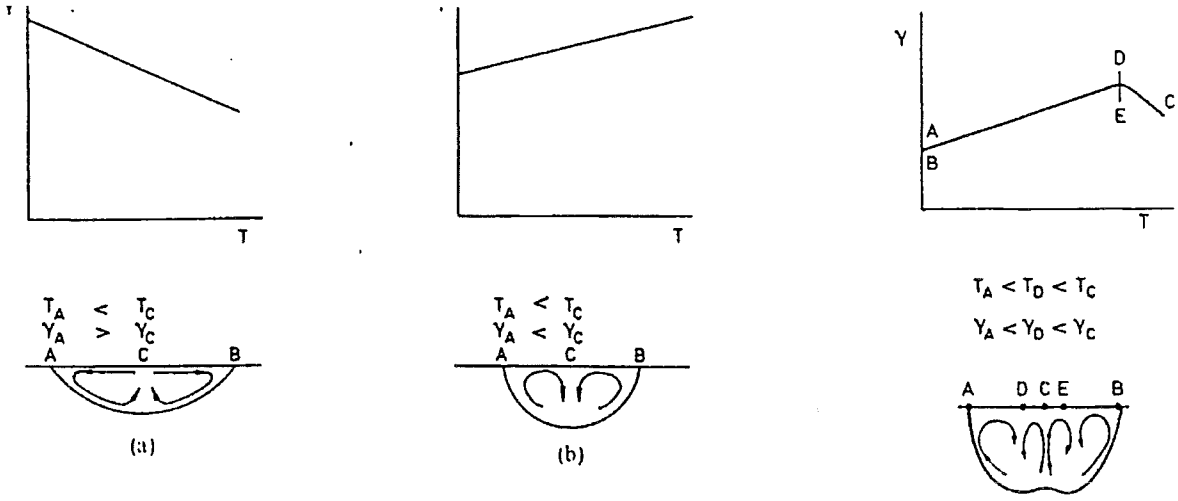

Fig. 2.6. The effects of the surface tension temperature gradient over the weld pool on the shape of the weld pool:
a and b. As suggested by Heiple and Roper [18]
c. As suggested by Keene [19].

Marangoni force

A second effect that influences the weld pool flow pattern is that of surface tension gradient [22]. A thermocapillary flow, also called Marangoni flow, is induced by this gradient which exerts a force on the fluid metal in the direction of higher surface tension. A large temperature gradient at the surface of the weld pool implies a large surface tension gradient and thus a strong driving force. Surface tensions of metals have different temperature coefficient, varying from negative to positive. Pure metal has a negative surface tension temperature coefficient. Hot metal at the centre moves outward to the side of the weld pool, as a flow of type A. As a consequence, the weld pool is wide and shallow penetration is obtained. Small additions of surface-active elements, like oxygen or sulphur, lower the surface tension of the base material when its temperature is near melting point. This is the case at the edge of the weld pool. Higher temperature reduces the influences of elements on the surface tension till at a critical temperature the elements are no longer surface-active. This means that a positive surface tension temperature gradient is formed. Molten metal at the surface flows from the edges to the centre of the weld pool surface as type B. When the temperature of the weld pool underneath the arc is higher than the critical temperature a local outward flow will occur [21], as shown in Fig. 2.6.

Drag force

During welding arc plasma flows outward over the surface of the weld pool. Aerodynamic drag forces act upon the molten metal and imply an outward directed flow, type A. The drag forces increase with increasing arc length [15].

Buoyancy force

Temperature variation in the weld pool causes variation in density of the molten metal. Near the edges of the weld pool the molten metal is cooler and has a higher density than metal at the centre of the weld pool. Buoyancy force causes the metal near the edges to sink while it moves upward at the centre, resulting in a flow of type A, Fig. 2.5. Under normal welding conditions the buoyancy force does not play an important role as long as the depth of the weld pool is less than 10 mm [23].

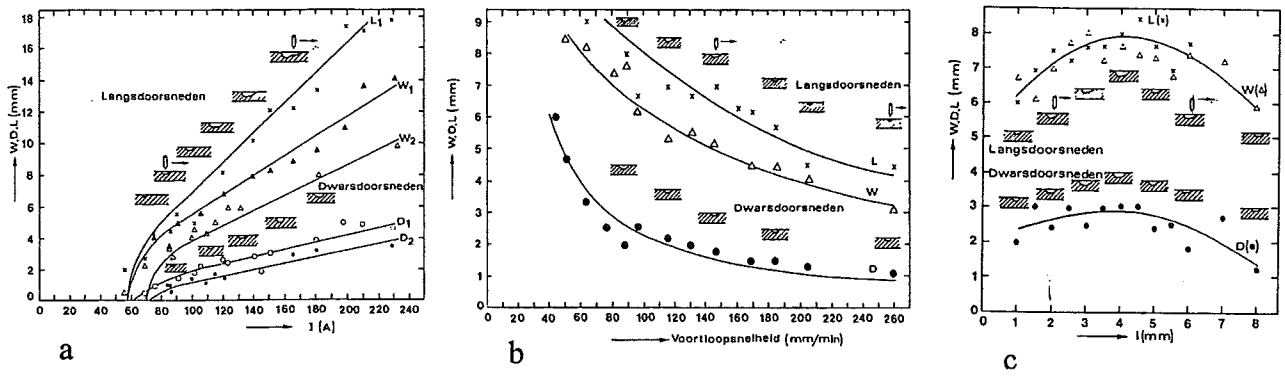

Fig. 2.7. Changes in weld pool dimensions (width W, depth D, length L)[26]as a function of:

a. welding current
b. travel speed
c. arc length

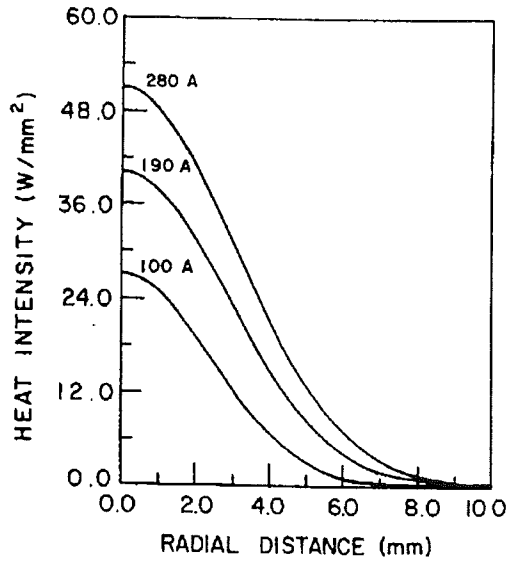

Fig. 2.8. The heat distribution at various current [6].

2.3.2 Welding parameters

Several factors influence the magnitude of the forces acting on the weld pool. For example, the composition of the workpiece can affect the surface tension temperature coefficient. The area of the anode root determines the current density and the heat flux density. Also the arc pressure is important while it determines the strength of drag forces across the weld pool surface. Several changes in weld pool flow are primarily a result of varying parameters like welding current, arc length and travel speed. Changes in the width, depth and length of weld pool as function of the welding parameters for austenitic stainless steel (AISI 304) under GTA-welding conditions were collected by Franse et al. [24] and are shown in Fig. 2.7.

Welding current

An increase in welding current enforces both the Lorentz flow and the drag force, causing a deeper and wider weld pool. It also affects the heat input to the workpiece, as was shown in eq. (2.2). The heat distribution for different levels of welding current is shown in Fig 2.8 [6]. Higher current causes both higher peak intensity and wider heat distribution. This induces a larger temperature gradient at the surface of the weld pool, which enforces the Marangoni flow. This alters the weld pool dimensions when the overall flow pattern is governed by Marangoni flow. For steel with negative surface tension temperature coefficient, the weld penetration will become smaller because the outward directed flow is amplified. For steel with a positive surface tension temperature coefficient the opposite occurs [18].

Travel speed

Increasing the travel speed decreases the heat input per unit length, but does not change the heat input distribution. Modelling the heat conduction in the workpiece showed that welds travelling at low speed exhibit a steeper temperature gradient and a higher peak temperature on the surface. For Marangoni controlled flow an increase in penetration is expected with decreasing travel speed for materials with a positive surface tension temperature coefficient [18].

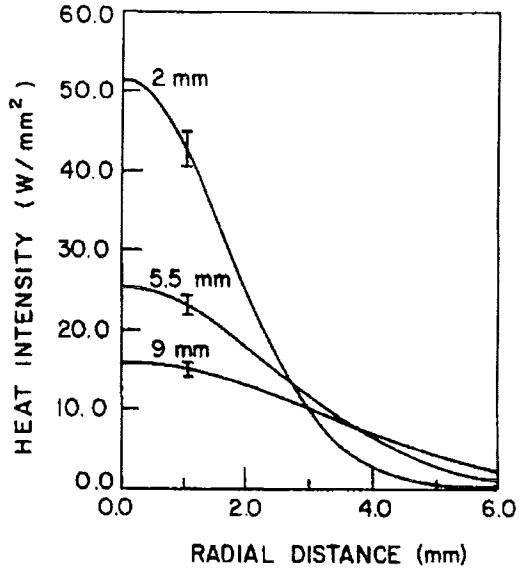

Fig. 2.9. The heat distribution at various arc length [6].

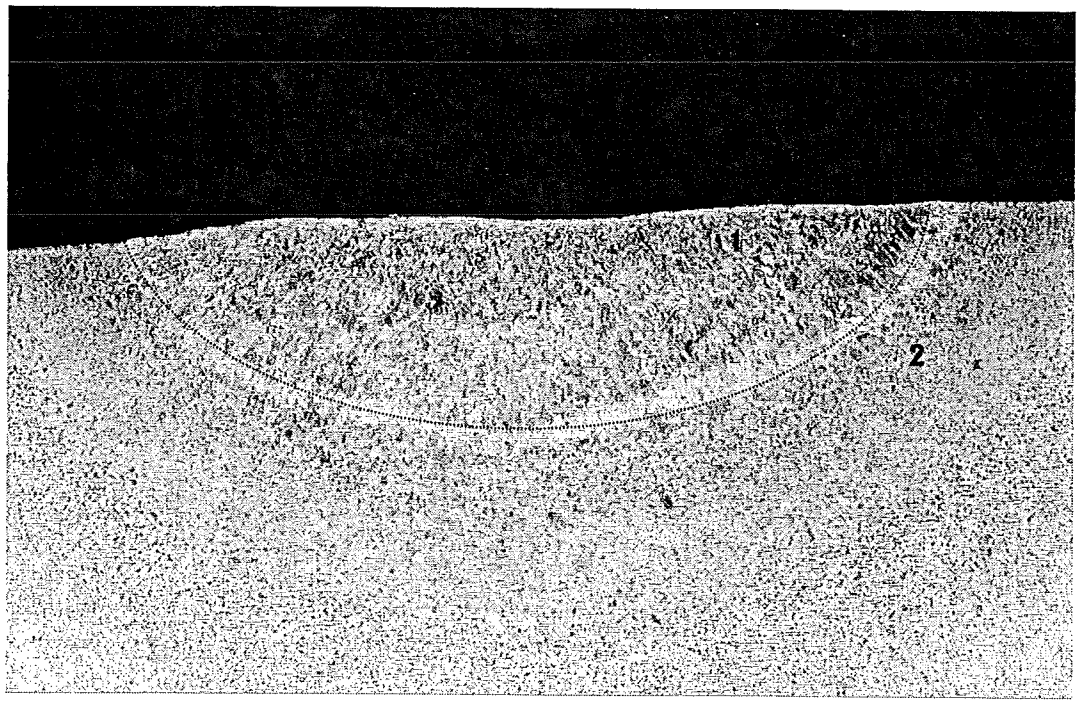

Fig. 2.10. Cross-section of weld.
1. fusion zone
2. HAZ
--- fusion boundary

Arc length

Changing the arc length has several effects on the welding arc. When the distance between electrode and workpiece is increased and current is kept constant the arc voltage increases. A higher voltage corresponds with higher arc energy. However, an increase in arc length also reduces the process efficiency. Changes in heat distribution as function of the arc length is shown in Fig. 2.9. With larger arc length a broader anode root is formed. Under normal welding conditions the anode root increases linearly with the arc length [6]. Broadening of the heat input induces a lower temperature gradient with increasing arc length and consequently a decrease in Marangoni flow [18].

2.3.3 Structural changes

During the welding process part of the workpiece melts and again solidifies. Consequently, the structure of this part will be different from the rest of the workpiece. Material near the melted zone temporarily experiences a large temperature increase, which influences the grain structure as well. These two zones are called the fusion zone and the heat-affected zone (HAZ), respectively. They can be easily distinguished by their grain structure, as shown in Fig. 2.10.

Fusion zone

In the fusion zone all metal is melted by the heat input of the arc. When the metal solidifies crystals are nucleated on solid crystals located at the solid-liquid interface, known as epitaxial growth. Grains grow parallel to the maximum temperature gradient and have the same orientation as the grains they started from [16]. Some grains have a more advantageous orientation than others have, which results in difference of growth rate. These grains together form the primary structure of a weld.

In case of a moderate cooling rate, polygonal ferrite and grain boundary ferrite grow from grain boundaries into the austenite grains. Carbon will be expulsed from the ferrite into the austenite that becomes progressively enriched with carbon when the temperature falls. When the temperature drops below a certain value Widmanstatten ferrite is formed in the form of ferrite fingers or needles.

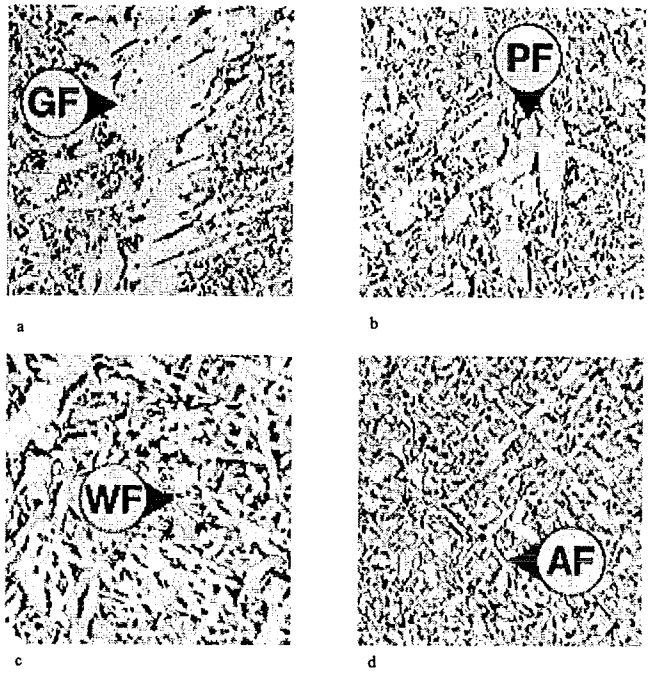

Fig. 2.11. Different ferrite appearances:
a. Grain boundary ferrite
b. Polygonal ferrite
c. Witmanstatten ferrite
d. Acicular ferrite

Finally acicular ferrite nucleates, which has a similar shape as Widmanstatten ferrite, except that its length-width ratio is smaller. Higher heat input decreases the fraction of acicular ferrite in the weld metal. Figure 2.11 gives an overview of the mentioned ferrite structures.

Heat-affected zone

The heat-affected zone is defined as the part of the base material that has been heated above a certain transition temperature, but that remained below the melting temperature. The microstructure of the heat-affected zone largely depends on the heat input and the distance from the fusion boundary. With increasing distance from the fusion boundary the local peak temperature decreases. High heat input increases the time that the metal is exposed to the peak temperature [25, 26].

Close to the fusion boundary the peak temperature is high and austenitic grain growth occurs. This results in the coarse-grained zone. The size of the grains depend on the time that zone experiences high temperature and thus on the heat input. Normally, this zone is very small and rarely observed. Adjacent is the fine-grained zone, where the peak temperature remained below the recrystallization temperature and no grain growth occurs. In the next zone, the intercritical zone, grain refinement occurs and further in the base material some spheroidization can be noticed.

2.3.4 Influences of additives

It appears that weld penetration of welds in stainless steel varies strongly with heat-to-heat variations. Heat-to-heat variations are a result of unavoidable composition changes between different batches of steel. This resulted in extensive research, which was focussed on the influences of minor composition changes on penetration properties of welds in stainless steel [18, 20-23, 27-29]. In this project carbon steel, Fe360, is used instead of stainless steel, but still the knowledge of forces acting on the weld pool and influences of welding parameters on the penetration can be applied.

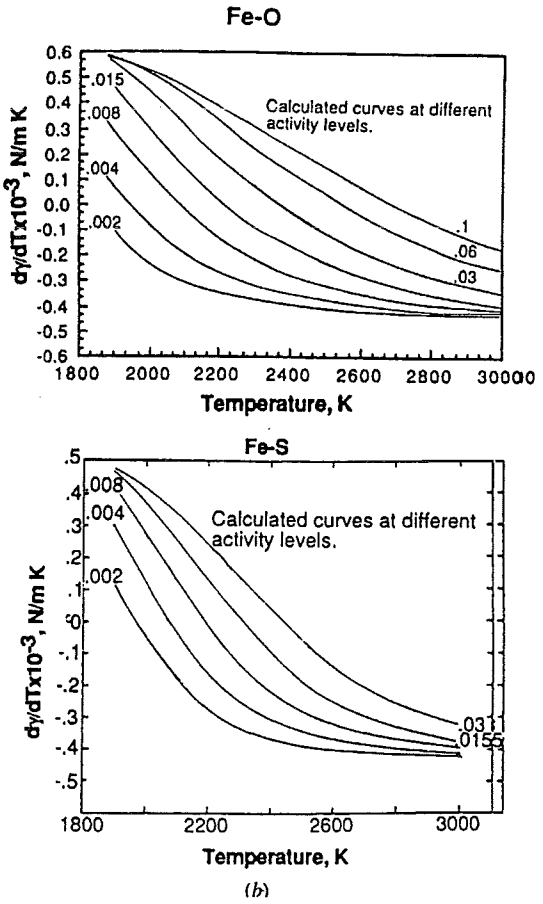

(b)

Fig. 2.12. Variations of surface tension temperature coefficient as a function of the composition and temperature [6].
a. Fe-O system
b. Fe-S system

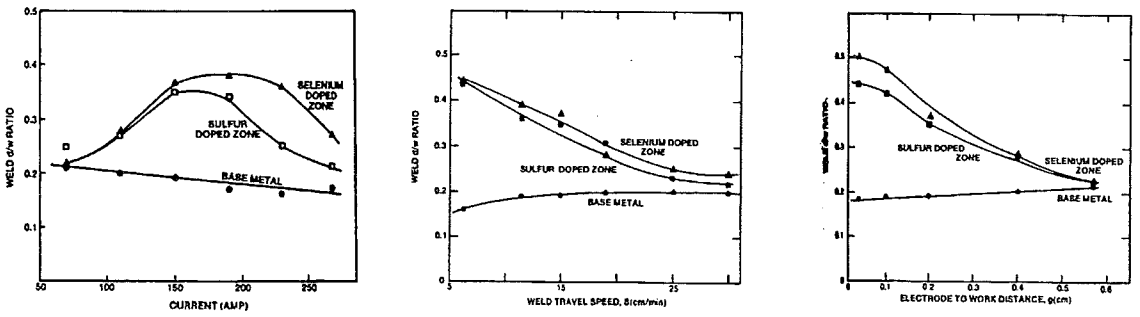

Fig. 2.13. Changes in D/W ratio [17] as a function of:
a. welding current
b. travel speed
c. arc length

In the previous section some theories about influences of additives on the welding arc were presented. To understand the influences of additives on the weld pool, researchers examined the effect of minor composition changes in the base metal on the weld pool formation. Minor composition changes have proven to alter the weld penetration in a significant way, especially in stainless steel when the concentration of surface-active elements, like sulphur and oxygen, varies.

The most satisfying theory for these results considers the Marangoni flow to be the dominant factor determining the penetration of the weld pool [22]. Surface-active additives alter the surface tension temperature coefficient thereby changing the Marangoni flow in the weld pool and thus the weld penetration. Variation of the surface tension temperature coefficient in binary systems (Fe-O and Fe-S) is determined by Sahoo [30], see Fig. 2.12. Clearly, the surface tension temperature coefficient changes with the concentration of oxygen or sulphur. It also diminishes with the temperature and changes from a positive to a negative value at high temperature. Results of D/W ratio measurements with varied sulphur and selenium concentration for different welding parameters can be explained with the Marangoni flow as dominant flow. The results are shown in Fig. 2.13 [22].

Not only the presence of surface active elements is important also the amount of elements that combine with surface active elements have to be considered. Several elements in steel have deoxidising properties, like Si, Mn and Al, or desulphurising properties, like Ca. According to the surface tension model these additives reduce the penetration properties of the steel because they diminish the amount of soluble oxygen or sulphur. This is confirmed for aluminium by D/W ratio measurements [28, 29]. Si did not always have a negative effect on penetration. This was thought to be caused by formation of manganese silicates, which float on the surface of the weld pool and have a positive effect on the arc characteristics [20].

The effect of the elements as described above were obtained in experiments where the elements were added to the workpiece by filling holes or slots and covering with an iron surface layer. When the additive is applied to the surface of the workpiece it causes additional effects on the arc behaviour, as was found by other researchers [1, 12, 14, 28, 31]. Arc constriction and arc trailing were already mentioned in the previous section. Variation in both arc and weld pool characteristics make the formation of the weld to a complex process.

2.4 Introduction to surface tension

The importance of the surface tension for the weld pool formation has been demonstrated in previous sections. In this section a short introduction to surface tension is given.

Atoms in the surface of a liquid undergo a stronger interaction with atoms in the bulk of the liquid than with atoms in the surrounding gas. As a result they are pulled into the bulk of the liquid. When new surface area is created a force is needed to counteract the attractive forces of the bulk. The force needed per unit of new created surface area is called surface tension.

Oscillation of the fluid causes changes in surface area. Therefore the oscillation frequency is a function of the surface tension of the fluid. During welding, the weld pool can be brought into oscillation with a pressure peak induced by a current pulse. A mathematical model [32-34] relates the natural oscillation frequency of the weld pool with the surface tension and the weld pool diameter. The frequency, f, in which a half-penetrated weld pool will start to oscillate, depends on the surface tension and the diameter of the weld:

$$f = 5.85 \left(\frac{\gamma}{\rho_l} \right)^{1/2} D^{-3/2} \qquad (2.5)$$

In this equation γ represents the surface tension [N/m], ρ_l the density of the liquid metal [kg/m^3] and D the diameter of the weld pool [m]. The depth and gravitational forces were found to have almost no influence on the frequency and are therefore not included in this equation.

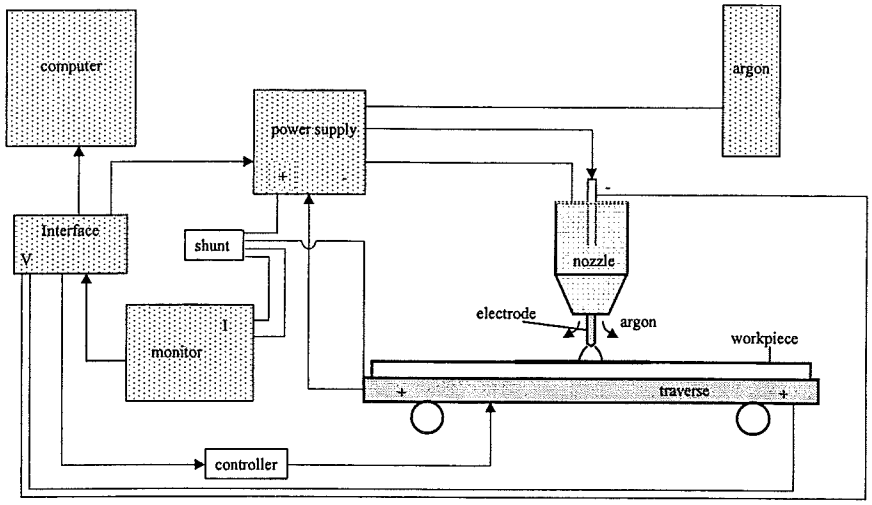

Fig. 3.1. Experimental set up for GTA welding.

Table 3.1. Standard welding conditions.

Workpiece material	Fe360, (200x250x10mm)
Electrode	W (2% ThO_2), 2.4 mm, 60°
Polarity	Negative electrode
Power supply	ESAB DTA 300
Shielding gas	Ar, 5 l/min
Welding current	180 A
Arc length	3 mm
Travel speed	2 mm/s

Table 3.2. Chemical composition of Fe360 measured with XRF and gasanalyses.

Element	wt %
Mn	0.65
Cu	0.26
Si	0.25
C	0.10
Co	0.08
Cr	0.08
S	0.041
Mo	0.02
Sn	0.02
As	0.01
Ni	0.01
P	0.01
Al	< 0.01
Nb	< 0.01
Ti	< 0.01
Va	< 0.01
Zr	< 0.01
Fe	98.4

3. Experimental procedure

3.1 Welding experiments

In this research project bead-on-plate experiments and blow-out experiments were carried out for both SiO_2 and Fe_2O_3. Three welding parameters were varied: the welding current, the travel speed and the arc length. The welding current was varied from 100 to 300 A in steps of 50 A, the travel speed was varied from 1 to 5 mm/s in steps of 1 mm/s and the distance between the workpiece and electrode was varied from 1 to 5 mm in steps of 1 mm. While one parameter was varied, the other parameters were kept constant at their standard value. In each situation arc voltage and weld pool dimensions were determined. Weld structure and hardness for the welds under standard conditions were also considered.

3.1.1 GTA-welding set-up

Bead-on-plate experiments were carried out on a standard GTA-welding set-up, as shown in Fig. 3.1. During the welding process plates were fixed on the traverse that moves underneath the electrode. The electrode consist of tungsten enriched with 2% ThO_2. A constant argon flow shields the arc and the weld pool from the surrounding atmosphere. The welding current and travel speed were both regulated by computer, which also measured the voltage during the welding process. The standard welding conditions are listed in Table 3.1.

3.1.2 Base material and additives

As workpiece Fe360 plates (200x250x10mm) were used. To enable comparison of the results, plates were taken preferably from the same heat in order to prevent influences of composition changes. However, due to the limited available amount of steel per heat two heats were used, one for the measurements with SiO_2 and one for the measurements with Fe_2O_3. The chemical compositions of both heats are listed in Table 3.2.

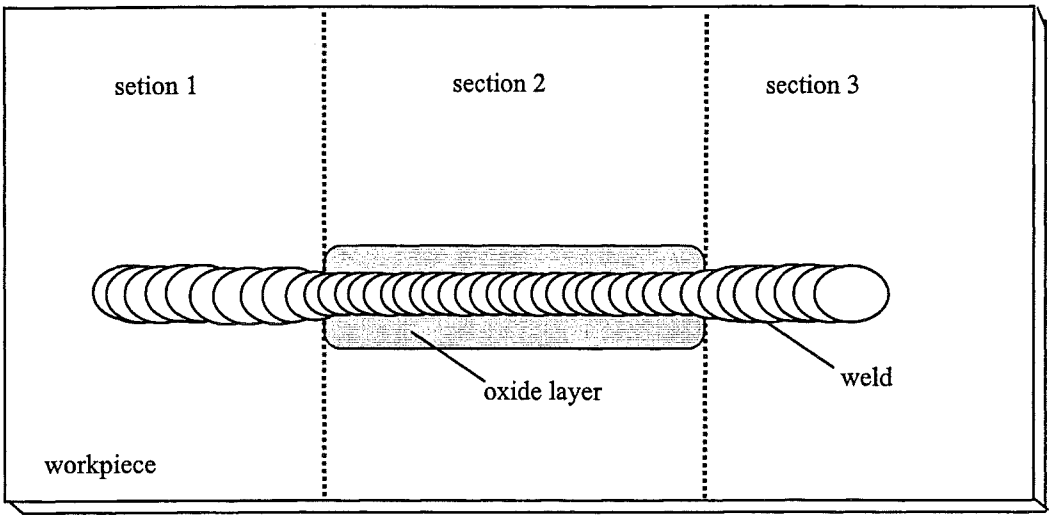

Fig 3.2. Topview of the workpiece.

The elements S, C and O were measured with gas analysis (Ströhlein OSA-Mat), while other elements were determined with X-ray fluorescence spectroscopy (Philips PW 1480).

Prior to welding the plates were ground and cleaned with acetone. The additive, SiO_2 or Fe_2O_3, mixed with acetone to a paste was applied with a brush. The additive was found to be sufficiently attached to withstand the flow of shielding gas and arc pressure.

3.1.3 Bead-on-plate experiments

The welds were performed on steel plates that were cleaned and covered with SiO_2 or Fe_2O_3. During one cycle the welding arc passes blank metal, without additive, section 1, with additive, section 2, and finally without additive, section 3, shown in Fig. 3.2.

After welding, transverse cross-sections were made of welds on blank steel and welds with additive. After grinding, polishing and etching with 1% Nital the samples were ready for further measurements. Of each cross-section the depth (D), the width (W) and the cross-sectional area (A) of the weld were measured using optical microscopy (Jenavert microscope in combination with Leica Imaging systems).

3.1.4 Blow-out experiments

To determine the dimensions of the weld pool during the welding process blow-out experiments were carried out. When the arc was extinguished, the molten metal was immediately blown out of the weld pool by an argon gas flow. These experiments were performed on blank steel and with additive. Length and width were measured with a movable crosshead.

3.2 Surface tension measurements

Surface tension measurements were carried out for SiO_2 as additive. The experimental set-up is presented in this section together with other important welding conditions.

3.2.1 Experimental set-up

Surface tension measurements were carried out to determine the surface tension temperature coefficient of liquid steel and of liquid steel with SiO_2 as additive. Therefore the oscillation frequency of the weld pool is measured during bead-on-plate experiments with a pulsed welding current. The computer controlled the current input and measured the voltage oscillations. The duration of the current pulse is 4 ms and its height is 100 A above the base current. The temperature of the weld pool was measured with an infrared radiation pyrometer (fabricated by L.I.E.) directly after extinction of the arc. The pyrometer has a response time of 60 ms and a spot diameter of 3 mm. The temperature is converted into a voltage signal which was transmitted to the computer.

3.2.2 Surface tension measurements

The surface tension experiments were carried out during bead-on-plate welds under traveling conditions. The weld pool oscillation is triggered with a short current pulse on top of the base current. The oscillation of the weld pool causes the arc length and thus the arc voltage to change with time. The frequency is extracted from the collected arc voltage data.

The width of the weld pool was measured afterwards with a movable crosshead. When the weld pool did not have a circular but an elongated shape, an equivalent width was calculated that, when the weld pool would be circular, resulted in a comparable surface area. The surface tension was then calculated with eq. 2.5.

The base current was varied in order to vary the temperature of the weld pool. The pyrometer was focused slightly behind the centre of the weld pool as the electrode forms a barrier for direct measurements. It must be noted that a strong temperature gradient exists within the weld pool. Therefore measurements of the pyrometer can only be considered as a relative indication for the general weld pool temperature.

3.3 Hardness measurements and structure of the weld

Vickers hardness testing were carried out on the cross-sections of the welds. In Vickers hardness test uses a square base pyramid is used to indent the metal surface with a certain load. The strength of the metal is indicated by the Vickers hardness number, which is defined as the load divided by the surface area of the indentation. The test is described in ASTM Standard E92-72 [35]. The Vickers hardness measurements were carried out for the welds made under standard conditions, without and with additives.

For analysing the weld, structure photographs were taken of the cross-sections of a weld under standard conditions and of welds with SiO_2 or Fe_2O_3 as additive. Three areas in the weld were examined: the fusion zone, the fusion boundary and the heat-affected zone. The microscope used was a Neophot 30.

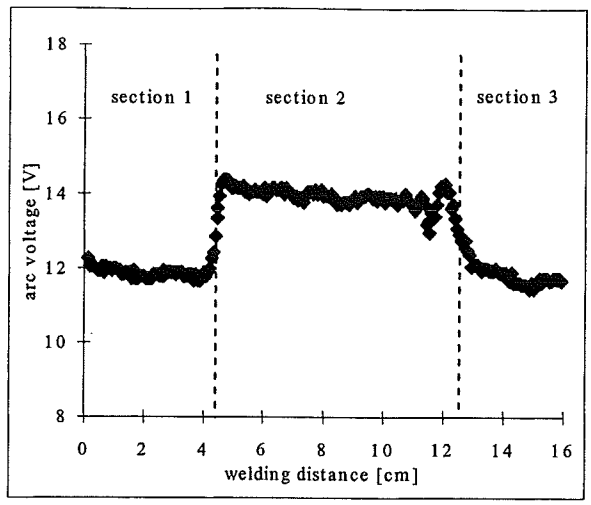

Fig. 4.1. Arc voltage behaviour during the welding process with SiO_2 added on the surface of the plate in section 2 (I = 180 A, v = 2 mm/s, l = 3 mm).

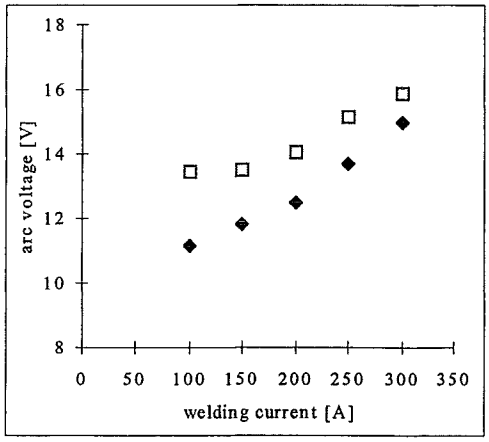

Fig. 4.2. Arc voltage as a function of welding current for steel without SiO_2 (♦) and for steel with SiO_2 (□).

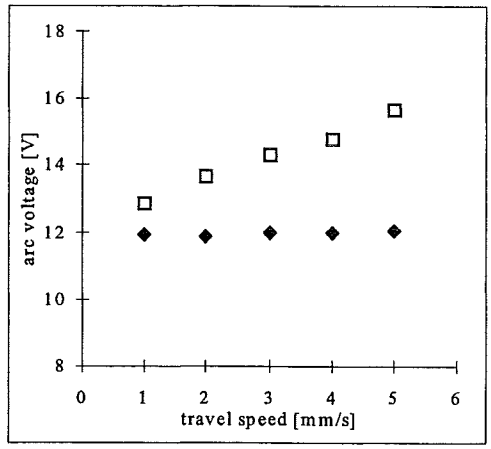

Fig. 4.3. Arc voltage as a function of travel speed for steel without SiO_2 (♦) and for steel with SiO_2 (□).

4. Results and discussion

In this chapter experimental results are presented and discussed. Influences of the additives SiO_2 and Fe_2O_3 are described in sections 4.1 and 4.2. For each additive, first changes in the welding arc are discussed followed by changes in the weld pool. Then changes in composition, hardness and weld structure are presented.

4.1 Influences of SiO_2

4.1.1 Changes in the welding arc

A thin layer of SiO_2 was applied to a part of the surface of the workpiece before welding. When the welding cycle was started and the arc reached the oxide layer visible constriction of the arc was observed. The arc voltage was measured continuously during the experiments and is shown in Fig. 4.1. In the region with SiO_2 present on the surface of the plate, the voltage increased with 2 to 3 V (ca. 20%). For a better understanding of the arc behaviour the changes in arc voltage were determined for different values of the welding current, travel speed and arc length.

Influence of welding current

The welding current was changed from 100 to 300 A in intervals of 50 A. The arc voltage for blank steel and with SiO_2 as function of the welding current are shown in Fig. 4.2. It can be seen that the arc voltage increases with increasing current for both types of welds. It is clear that with increasing current the differences between welds on blank steel and with SiO_2 diminish.

Influence of travel speed

The travel speed was varied from 1 to 5 mm/s in intervals of 1 mm/s. Changes in arc voltage as function of travel speed are shown in Fig. 4.3. On blank metal the voltage does not change significantly, while for welding with SiO_2 the arc voltage is higher and increases with increasing travel speed. This results in an increase in difference between both types of welds with increasing travel speed.

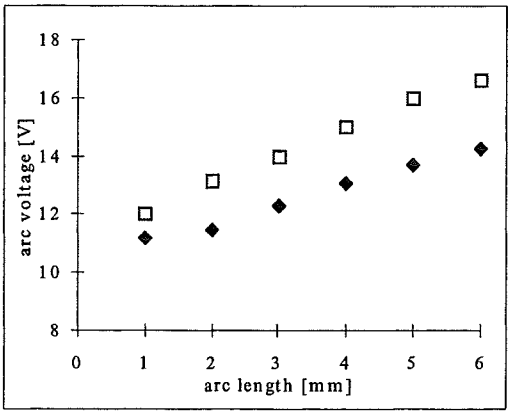

Fig. 4.4. Arc voltage as a function of arc length for steel without SiO_2 (♦) and for steel with SiO_2 (□).

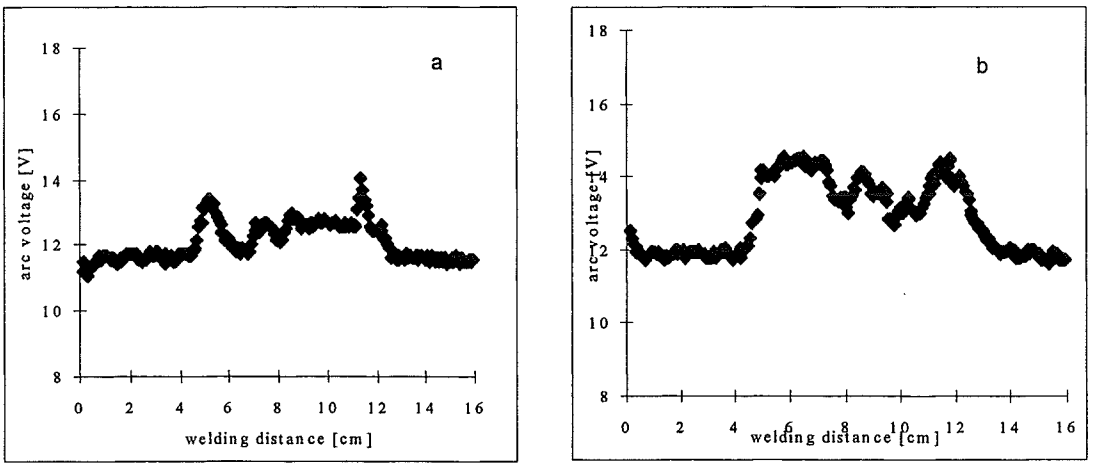

Fig. 4.5. Arc voltage behaviour during the welding process with SiO_2 added in a) normal quantity, b) large quantity.

Influence of arc length

The arc length was changed from 1 to 6 mm in steps of 1 mm. The influence of SiO_2 on arc voltage as a function of arc length is shown in Fig. 4.4. The voltage increases about linearly with increasing arc length. With SiO_2 applied on the surface a higher voltage was found and the voltage increased faster with increasing arc length than for a blank plate.

Discussion of results

The experimental results of the arc voltage measurements as presented in the foregoing are similar to those found by Middel [1]. Under all circumstances the arc voltage increases when SiO_2 is added. This effect can be quantitatively explained with the mechanism of arc constriction as a result of the presence of vaporised additive in the outer regions of the arc, see section 2.2.3.

The smaller voltage increase at high welding current (300 A) coincides together with a visual decrease in arc constriction. A comparable result was found by Kazakov [14] who stated that at high current the amount of vaporised additive present in the arc is diminished strongly by high plasma flow speed. A higher current induces a larger electromagnetic force in the arc, thereby increasing the flow speed. Consequently, vaporised additives are removed from the arc at a faster rate, resulting in a smaller voltage increase and less arc constriction.

If indeed the degree of arc constriction is a function of the amount of additive present in the arc, the thickness of the oxide layer should influence the arc voltage. Additional experiments were performed in which the voltage with a normal oxide layer was compared with that of a thick layer. Figure 4.5 shows that the arc voltage increase was larger for a thick layer of SiO_2, supporting this theory. Part of the voltage increase with increasing travel speed can be a result of the larger amount of SiO_2 that is vaporised per time unit.

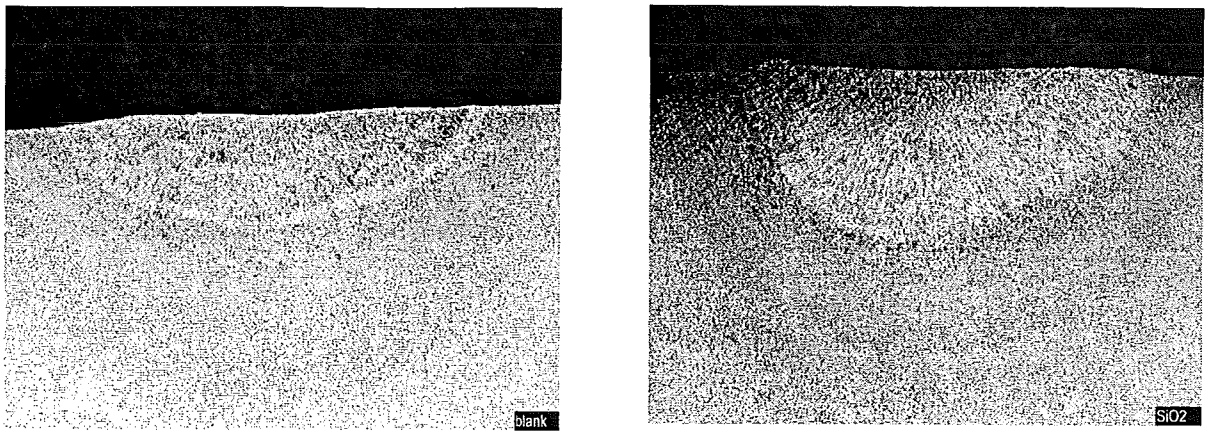

a b

Fig. 4.6. Transverse cross-sections under standard welding conditions.
a. blank steel
b. with SiO_2

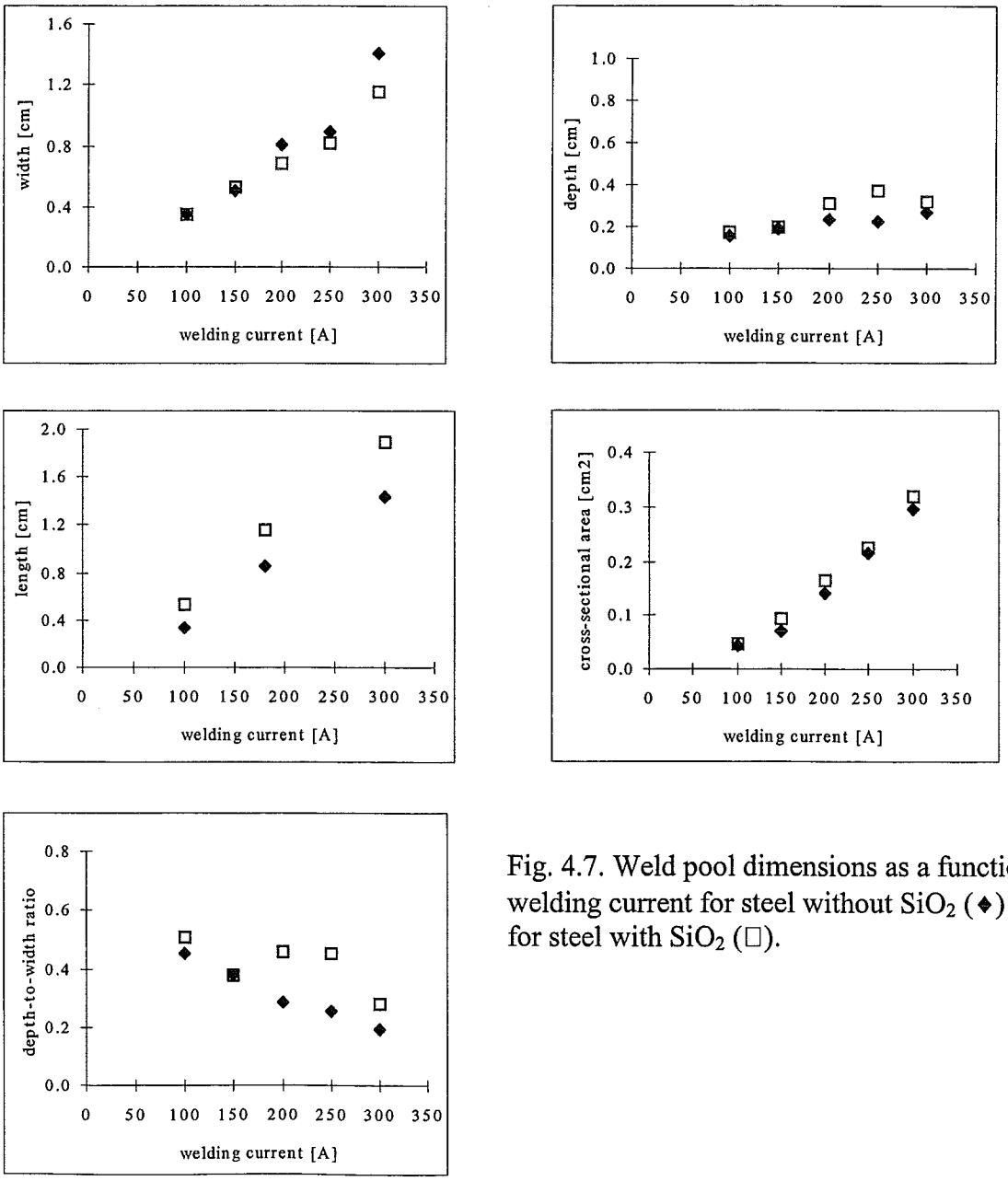

Fig. 4.7. Weld pool dimensions as a function of welding current for steel without SiO_2 (♦) and for steel with SiO_2 (□).

Besides arc constriction another effect, arc trailing, influences the arc voltage, see section 2.2.3. Figure 2.3 shows that the effective arc length in the presence of SiO_2 is 1 à 2 mm larger than the normal arc length. From Fig. 4.4 it is concluded that arc voltage increases about 0.5 V per mm arc length. This means that arc trailing can account for a voltage increase of 0.5 à 1 V at a travel speed of 4 mm/s. Under standard welding conditions the effective arc length was found to increase 0.3 mm, in this way accounting for a smaller voltage increase. Arc trailing is thought to diminish with increasing current while the arc becomes stiffer at high current. Visual observation confirmed this. However, no photographs are available for a more accurate determination. With increasing arc length an increase in arc trailing is expected.

4.1.2 Changes in the weld pool

In Fig. 4.6 two transverse cross-sections are shown obtained with and without SiO_2. Both welds are made under standard welding conditions. Significant changes in shape and size of weld pool are noticed after welding with SiO_2. A deeper and narrower weld pool is formed with a larger cross-sectional area compared to the weld on blank steel.

Influence of welding current

Variations in width, depth, depth-to-width ratio, length and cross-sectional area of the weld pool with changing current for welding on blank steel and with SiO_2 are shown in Fig. 4.7. The width, depth, length and cross-sectional area of welds on blank steel all increase with increasing current. The width increases more than the depth, which causes a decrease in depth-to-width ratio with increasing current.

With SiO_2 the width also increases with increasing current but not as fast as for welds on blank steel. The depth is generally larger than for welds on blank steel. A significant increase in length of the weld pool was found, which increases with increasing welding current. The D/W ratio for the welds with SiO_2 is larger than for the welds on blank steel, especially at 200 or 250 A. The cross-sectional area is slightly larger compared to the cross-sectional area of blank steel.

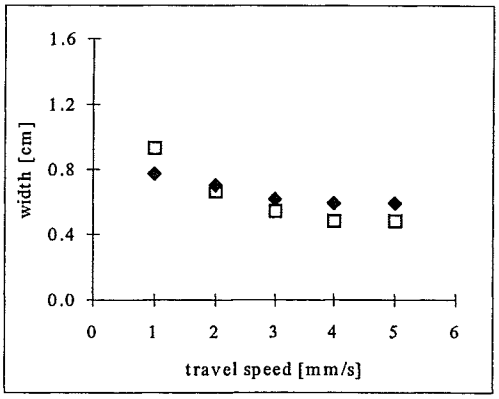

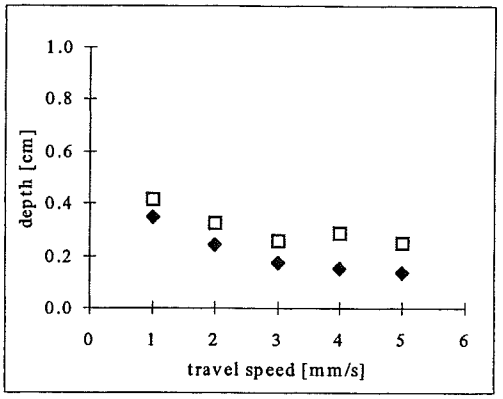

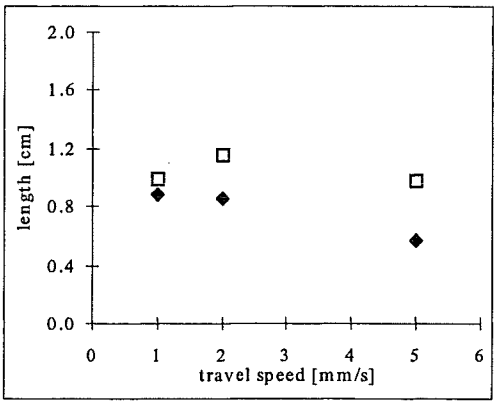

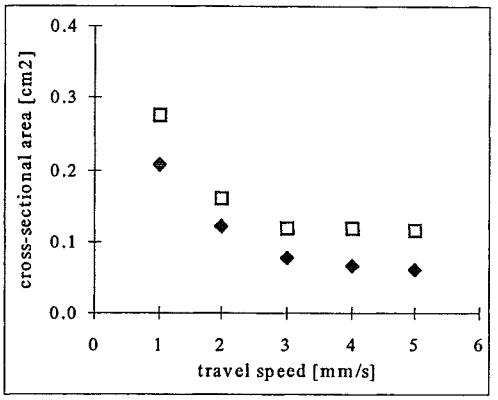

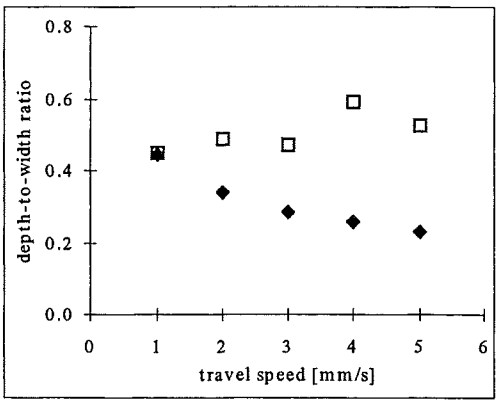

Fig. 4.8. Weld pool dimensions as a function of travel speed for steel without SiO_2 (♦) and for steel with SiO_2 (□).

Influence of travel speed

Variations of the width, depth, depth-to-width ratio, length and cross-sectional area of the weld pool with changing travel speed for welding on blank steel and with SiO_2 are shown in Fig. 4.8. Width, depth, D/W ratio and length for welds on blank steel decrease with increasing travel speed.

With SiO_2 the width is generally smaller than for blank steel, whereas the depth is larger. The D/W ratio is also larger, and the difference between the two types of welds increases with increasing travel speed. The length is also larger and the difference between the welds increases with increasing travel speed. The area of cross-section for welds with SiO_2 added is larger than for blank steel.

Influence of arc length

Variations of the width, depth, depth-to-width ratio, length and cross-sectional area of the weld pool with changing arc length for welds on blank steel and with SiO_2 are shown in Fig. 4.9. The width and length of the weld pool remain almost constant, while cross-sectional area, depth and also D/W ratio slightly decrease with increasing arc length.

With SiO_2 the width is slightly smaller than for blank steel and it remains constant with increasing arc length. The depth and length of the weld pool are larger than for blank steel and also show no significant variation with increasing arc length.

Discussion of results

For welds on blank steel identical relationships between width, depth and length with the welding parameters were found by Franse [24]. For welds with SiO_2 constriction of the arc by negative ions could be a logical explanation for the larger depth and smaller width. The constricted arc increases the current density at the arc-pool interface and thus enforces the Lorentz flow in the weld pool. This flow is inward directed and favours a deep and narrow weld pool, also mentioned in section 2.3.1.

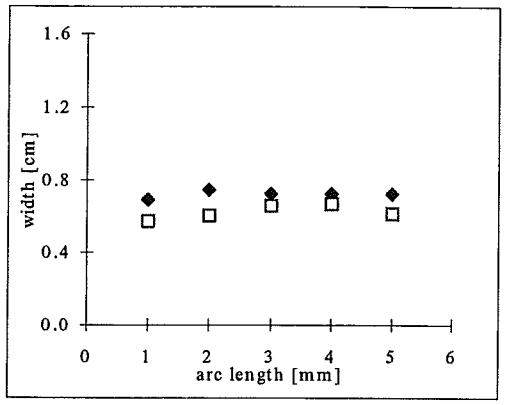

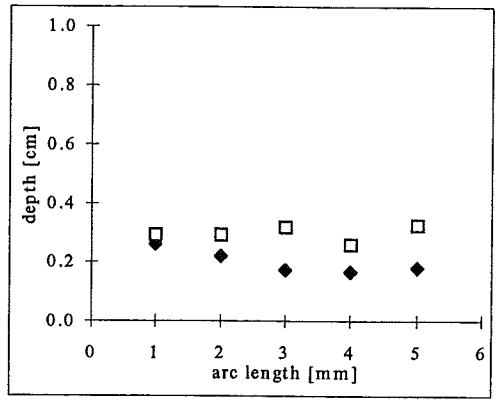

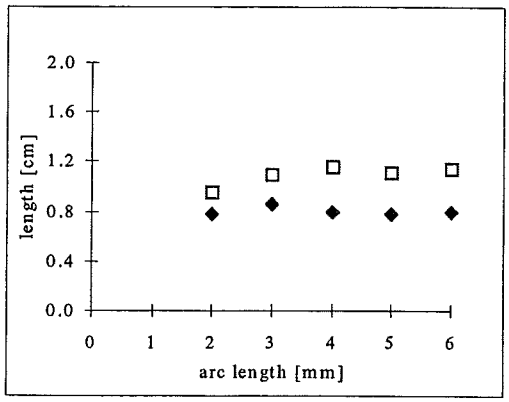

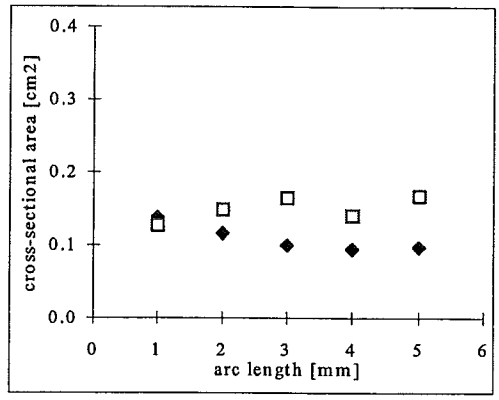

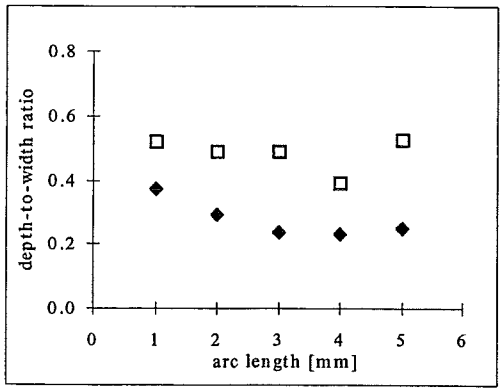

Fig. 4.9. Weld pool dimensions as a function of arc length for steel without SiO_2 (♦) and for steel with SiO_2 (□).

However, when changes in weld pool dimensions as function of the welding current are considered, it appears that contrary to the effect of SiO_2 on arc voltage, the effect on width, depth and length does not diminish with increasing welding current. Therefore, other effects that influence the weld pool formation should be considered.

As stated before, the oxide layer has a considerable influence on the behaviour of the arc. Visual observation of the welding process gives the impression that part of the additive is floating on top of the weld pool in the cooler outer regions. Apparently, the presence of this layer causes the arc root to constrict perpendicular and elongate parallel to the welding direction. This explains the significant difference in width and length of weld pool with and without SiO_2.

The presence of the oxide layer explains why with increasing arc current the changes in arc voltage diminish but the changes in weld pool dimensions increase. At higher current a wider arc is formed and more oxide becomes involved in the welding process, which increases the influence of SiO_2 on the width of the weld pool.

The increase of the influence of SiO_2 on the width and length of the weld pool with increasing travel speed is also a result of the presence of the oxide layer. Because the arc root gets less chance to push the oxide to the edge of the weld pool a more effective arc root constriction is obtained. This explains the smaller width and larger length of the weld pool at high travel speed.

So far most of the results can be explained with arc constriction and the presence of a molten oxide layer on the surface of the weld pool. However, the effect on the depth strongly diminishes at a welding current of 300 A, which is not expected with the previous considerations. This change indicates that the Marangoni flow also has to be taken in consideration. For the weld with SiO_2 a positive surface tension temperature coefficient is expected, resulting in an inward directed flow. At that high temperature (induced by high current) surface active elements loose their influence on the surface tension of the weld pool, as mentioned in section 2.3.1. Therefore, a locally outward directed flow diminishes the depth of the weld pool.

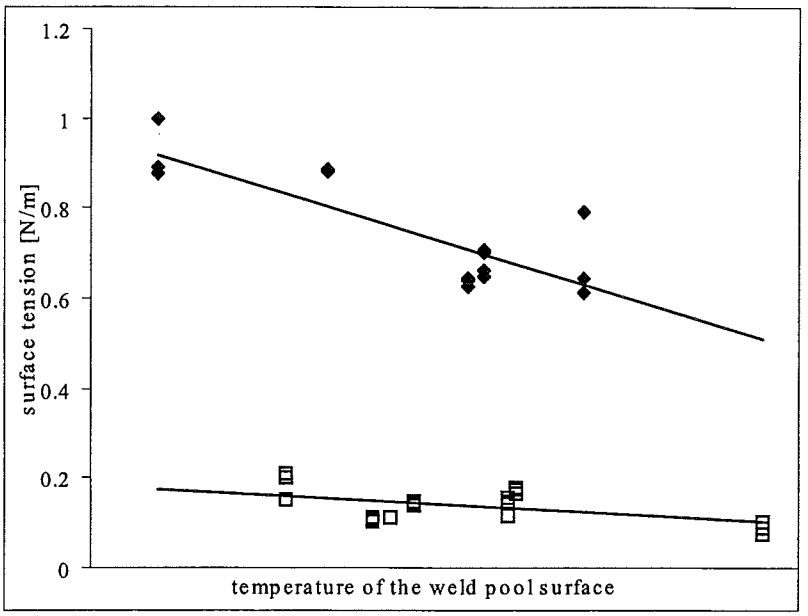

Fig. 4.10. Surface tension of the liquid metal as a function of temperature for steel without SiO_2 (♦) and for steel with SiO_2 (□).

4.1.3 Surface tension measurements

To determine the influence of SiO_2 on the surface tension temperature gradient, additional weld pool oscillation experiments were carried out as described in section 3.2.2. The natural oscillation frequency of the weld pool was measured after inducing the oscillation with a current pulse on top of the welding current. Some difficulties arose in measuring the oscillation frequency at low current (<180 A) because too much back round noise prevented accurate measurements. Therefore, surface tension could only be determined for higher current and thus higher temperature. Because the pyrometer did not give the precise temperature, as discussed in section 3.2.2, the output of the pyrometer was used as a relative indication for the temperature of the weld pool. By substituting the measured oscillation frequency and diameter into eq. 2.5 the surface tension was calculated. For the density of the liquid metal a value of 7000 kg/m^3 was used.

In Fig. 4.10 the calculated surface tension for welds on blank steel and welds with SiO_2 is plotted as a function of the temperature. Both curves have a negative slope and the curve for blank steel lies positioned considerably higher than that for steel with a layer of SiO_2. The value of the surface tension for blank steel in agreement with results obtained by Xiao and Den Ouden [33], who found a surface tension of 1.2 N/m for technical pure iron. With SiO_2 added the surface tension was expected to become lower due to a higher amount of oxygen in the weld pool, which is in agreement with the results. As mentioned in section 2.4 it was thought that oxygen would induce a positive surface tension temperature coefficient. Although the slope has become less steep than for blank steel it still contains a negative temperature coefficient. This can be understood when realising that at high temperature surface-active elements loose their influence on the surface tension, as mentioned by Keene [21]. Burgardt and Heiple [18] proposed that this effect is responsible for the decrease in D/W ratio at currents higher than 200 A. All experiments here were carried out with welding current higher than 200 A, which explains the negative surface tension gradient.

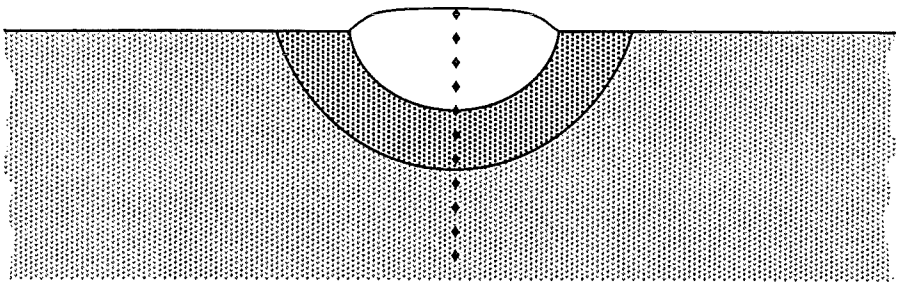

Fig. 4.11. Hardness measurements on the cross-section of a weld.

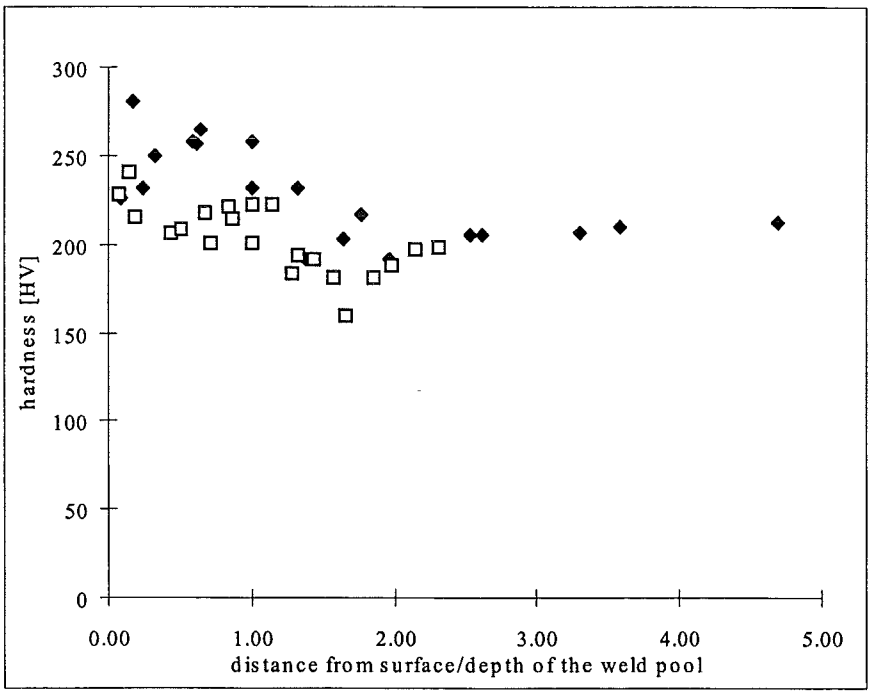

Fig. 4.12. Hardness measurements plotted against the relative depth for steel without SiO_2 (♦) and for steel with SiO_2 (□).

Although the surface tension measurements show large differences between the welds with and without SiO_2, it would be helpful to know the surface tension behaviour at lower temperature. Therefore the experimental set-up still has to be optimised. The shielding gas, argon, could be exchanged for helium, since helium has proven to increase the amplitude of the voltage oscillation, which would improve the distinction of the weld pool oscillation from the background noise.

Also accurate temperature measurements could be obtained by better positioning of the pyrometer and calibration with thermocouples.

Another option is to melt the steel in a cup instead of melting part of a plate, as was carried out for pure aluminium [34]. The steel can then be melted by induction heating, which excludes the influence of the welding current on the surface tension measurements. It is also to be expected that under these conditions the pool has a smaller temperature gradient and a fixed diameter. However, still some practical difficulties have to be solved. One of the difficulties is adding SiO_2 to the pool without loosing it by evaporation before measuring the oscillation frequency.

4.1.3 Hardness, structure and composition of the weld

The hardness of the weld was measured with Vickers testing equipment. The hardness was measured from the centre of the weld across the heat-affected zone into the base metal as shown in Fig. 4.11. The results for blank steel and for steel with SiO_2 are shown in Fig. 4.12. The hardness data are plotted on a relative scale, so that top of both welds and fusion boundaries coincide.

It is clear from Fig. 4.12 that the hardness of the welds obtained with SiO_2 is smaller than the hardness obtained with blank steel. This behaviour is presumably related to the thermal history of the metal. With SiO_2 added to the surface the weld pool elongates thus the weld metal remains longer at high temperature, hence experiencing a slower cooling rate. This explains the smaller hardness of the metal.

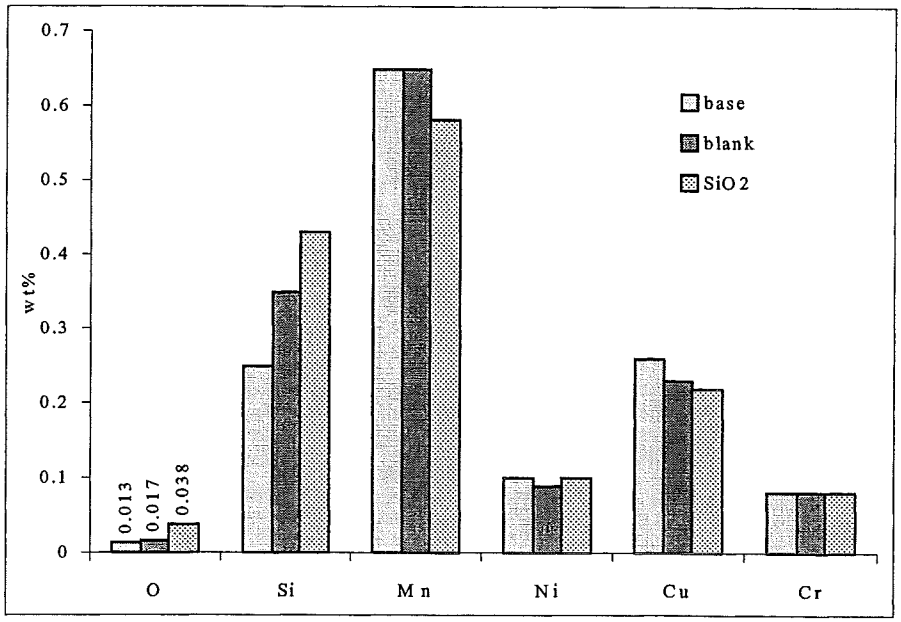

Fig. 4.13. Composition of the base material, weld metal and weld metal with SiO_2.

A second factor that influences the hardness is the chemical composition of the weld metal. Figure 4.13 shows the composition of a weld on blank steel and that of a weld with SiO_2, together with the composition of the base material. It appears that the amount of silicon in the weld metal increases when SiO_2 is used as an additive. Simultaneously, the amount of manganese decreases in the weld bead. The changes in the other elements are negligibly small. These changes in composition are not likely to influence the hardness of the metal considerably.

The increase in Si when SiO_2 is applied to the workpiece is not likely to be caused only by SiO_2 dissolved in the weld pool. Circa 0.2 gram per 10 cm of additive is applied on the surface of the plate before welding, which corresponds with 7 gram of weld metal. Consequently in the most extreme situation, when the total amount of the additive would be dissolved into the weld pool, an increase of 0.15 wt% of Si could be reached. The experiments show that a considerable part of the SiO_2 was left on the surface and thus a much smaller increase in Si would be expected. This indicates that the increase in Si is mainly caused by diffusion from the base metal.

Si and Mn are known to form manganese silicates that float on the surface of the weld pool. These have beneficial effects on the arc characteristics and increase the heat input and Lorentz forces [20], thereby improving the penetration. The decrease in Mn concentration as shown in Fig. 4.13, could be an indication that manganese silicates are formed. These silicates float on the surface and are expected to be lost during the preparation of the sample for chemical analysis. However, it is not observed that slag islands improve the arc characteristics. Better observation of the arc should be carried out to obtain more information of the influence of the manganese silicates.

The oxygen concentration is small and small changes are detected. In view of its effect on the surface tension especially the oxygen concentration at the surface of the weld pool is important. However, the measurement analysis technique determines the oxygen content of the bulk material and before measuring part of the surface is removed to prevent influences of oxidation of the surface. Therefore, the results should be interpreted with some caution.

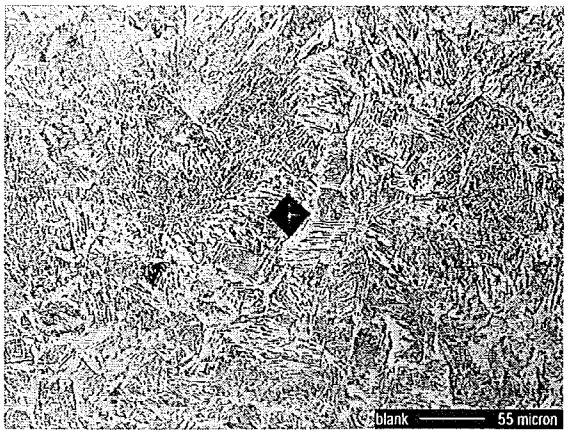

a

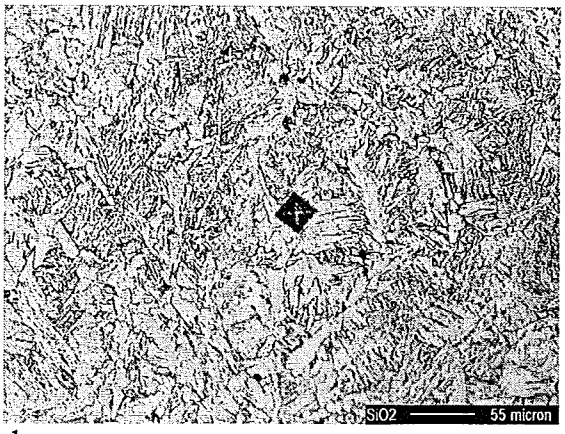

b

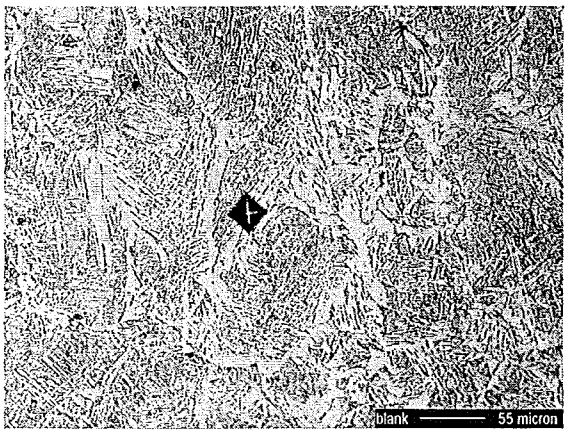

c

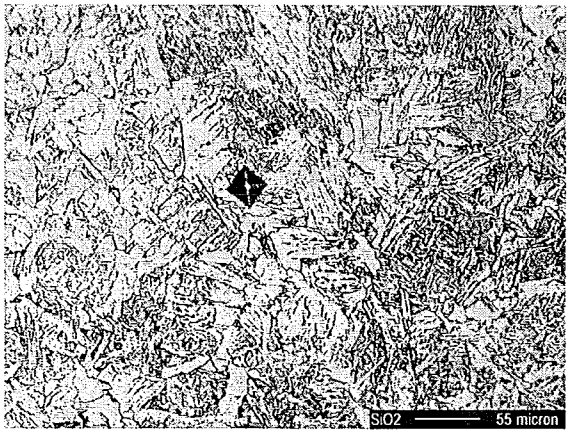

d

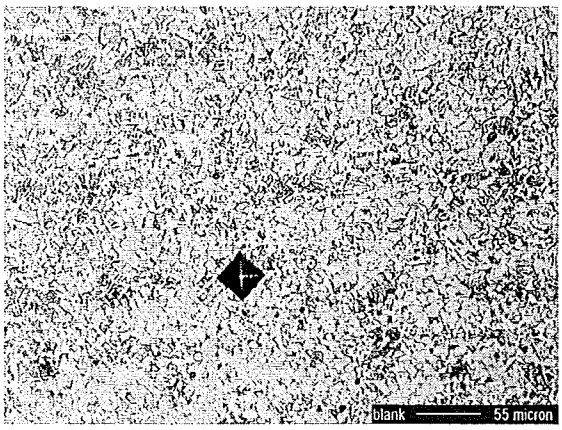

e

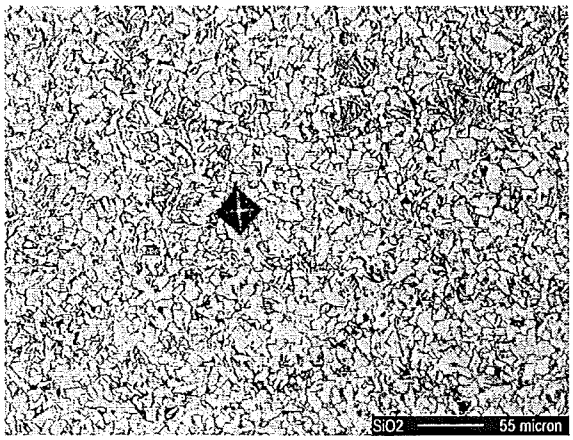

f

Fig. 4.14. Structures of the weld metal (a,c,e for blank steel, b,d,f for steel with SiO_2).
a and b. fusion zone
c and d. fusion boundary
e and f. HAZ

To examine the microstructure of the weld photographs were taken of the cross-section of the weld. Figure 4.14 shows photographs of the welds made under standard welding conditions with and without additive. The photographs were taken of different parts of the weld: the centre of the fusion zone, the fusion boundary and the heat-affected zone itself.

In the centre of the weld pool a certain amount of grain boundary ferrite is shown. Widmanstatten ferrite is present next to the grain boundary ferrite as ferrite plates. Furthermore, most of the area is filled with fine needles of acicular ferrite. With SiO_2 a coarser structure is shown. More grain boundary ferrite and Widmanstatten ferrite was formed. Also the acicular ferrite has a coarser structure.

At the fusion boundary the deviation of grain boundary ferrite indicates a coarser primary grain structure. Widmanstatten ferrite is present and again a reasonable large amount of acicular ferrite was formed. With SiO_2 more grain boundary ferrite and Widmanstatten ferrite are shown, together with coarse acicular ferrite.

The photograph of the HAZ shows a grain-refined structure with ferrite grains. For welds with SiO_2 the grains are slightly larger. Further, no large differences are noticed.

The increased amount of grain boundary and Widmanstatten-ferrite and the coarser structure of acicular ferrite when SiO_2 is added indicates that welds with SiO_2 experience a slower cooling rate than welds in blank steel. This is in agreement with the evaluation of the hardness of the weld.

4.2 Influences of Fe_2O_3

Experiments with Fe_2O_3 were executed on a different heat of mild steel than used for the experiments with SiO_2. In spite of small variations in composition, the results for blank metal are similar to those in the SiO_2 experiments. Therefore, the results of Fe_2O_3 and SiO_2 can be compared with each other.

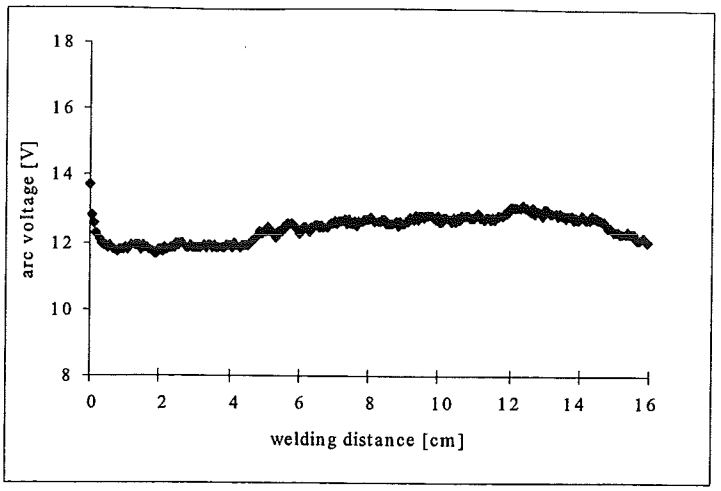

Fig. 4.15. Arc voltage behaviour during the welding process with Fe_2O_3 added on the surface of the plate (I = 180 A, v = 2 mm/s, l = 3 mm).

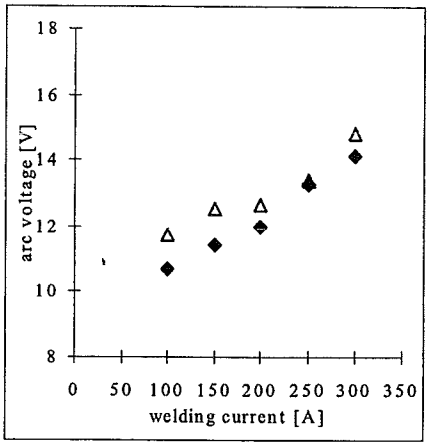

Fig. 4.16. Arc voltage as a function of welding current for steel without Fe_2O_3 (♦) and for steel with Fe_2O_3 (Δ).

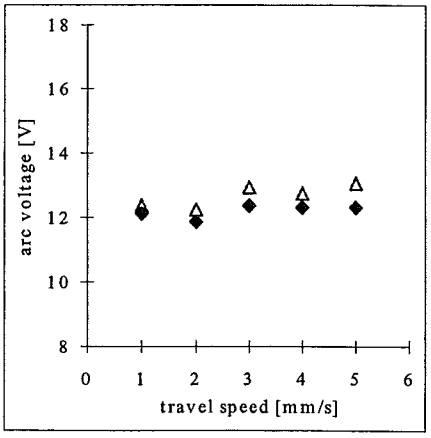

Fig. 4.17. Arc voltage as a function of travel speed for steel without Fe_2O_3 (♦) and for steel with Fe_2O_3 (Δ).

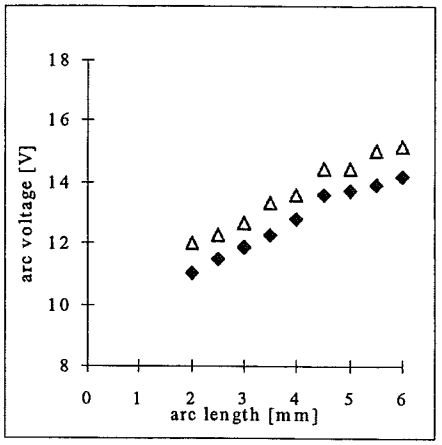

Fig. 4.18. Arc voltage as a function of arc length for steel without Fe_2O_3 (♦) and for steel with Fe_2O_3 (Δ).

4.2.1 Changes in the welding arc

Fe_2O_3 was applied to the surface of the plate in the same way as SiO_2. Visual observation of the welding process showed constriction of the arc when it had reached the oxide layer. However, constriction with Fe_2O_3 was found to be considerably smaller than the constriction observed with SiO_2. The behaviour of the arc voltage during the welding process is shown in Fig. 4.15. The weld was made under standard welding conditions. The voltage increase due to the presence of Fe_2O_3 was about 1 V (10%), which is considerably smaller than with SiO_2.

Influence of welding current

Changes in arc voltage as function of the current are shown in Fig. 4.16 for welds on blank steel and with Fe_2O_3. Differences between the curves are considerably smaller compared with welds with SiO_2 added, as was already noticed in Fig. 4.15. The effect of Fe_2O_3 on the arc voltage diminishes with increasing welding current, which was also found with SiO_2.

Influence of travel speed

Variations in arc voltage as a function of the travel speed are shown in Fig. 4.17. Only small differences in arc voltage were found between welds on blank steel and on steel with Fe_2O_3. This difference slightly increases with increasing travel speed.

Influence of arc length

Variations in arc voltage with arc length are shown in Fig. 4.18. A constant increase of 1 V was observed for all arc lengths when Fe_2O_3 was added. This is different from the results obtained with SiO_2, where the differences with blank steel in arc voltage was found to increase with increases arc length.

Discussion of results

The results described above clearly show that Fe_2O_3 has less influence on arc behaviour than SiO_2. Some arc constriction occurred but no arc trailing was noticed. Less arc constriction is in agreement with smaller difference in arc voltage between welds on blank steel and with Fe_2O_3. Changes in arc voltage as a function of welding

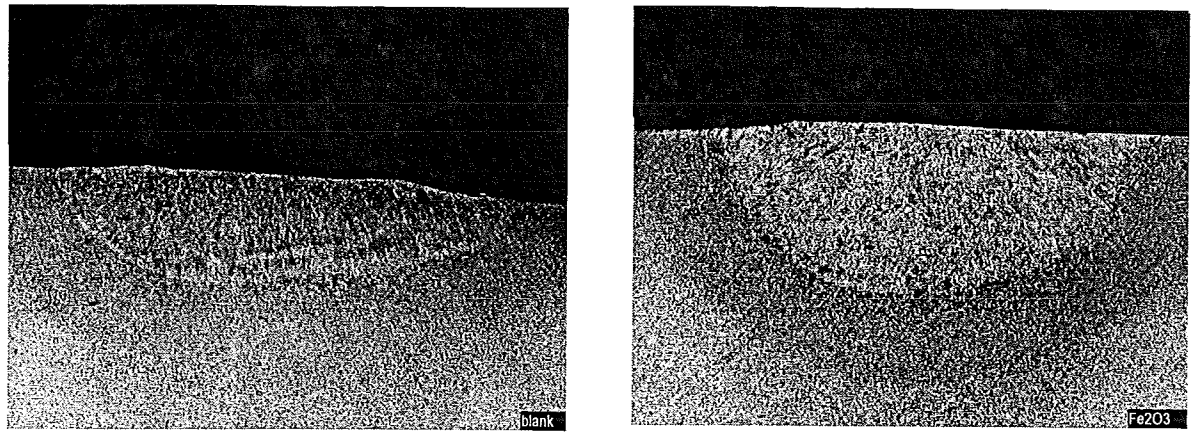

Fig. 4.19. Transverse cross-section under standard welding conditions.
a. blank steel
b. with Fe_2O_3

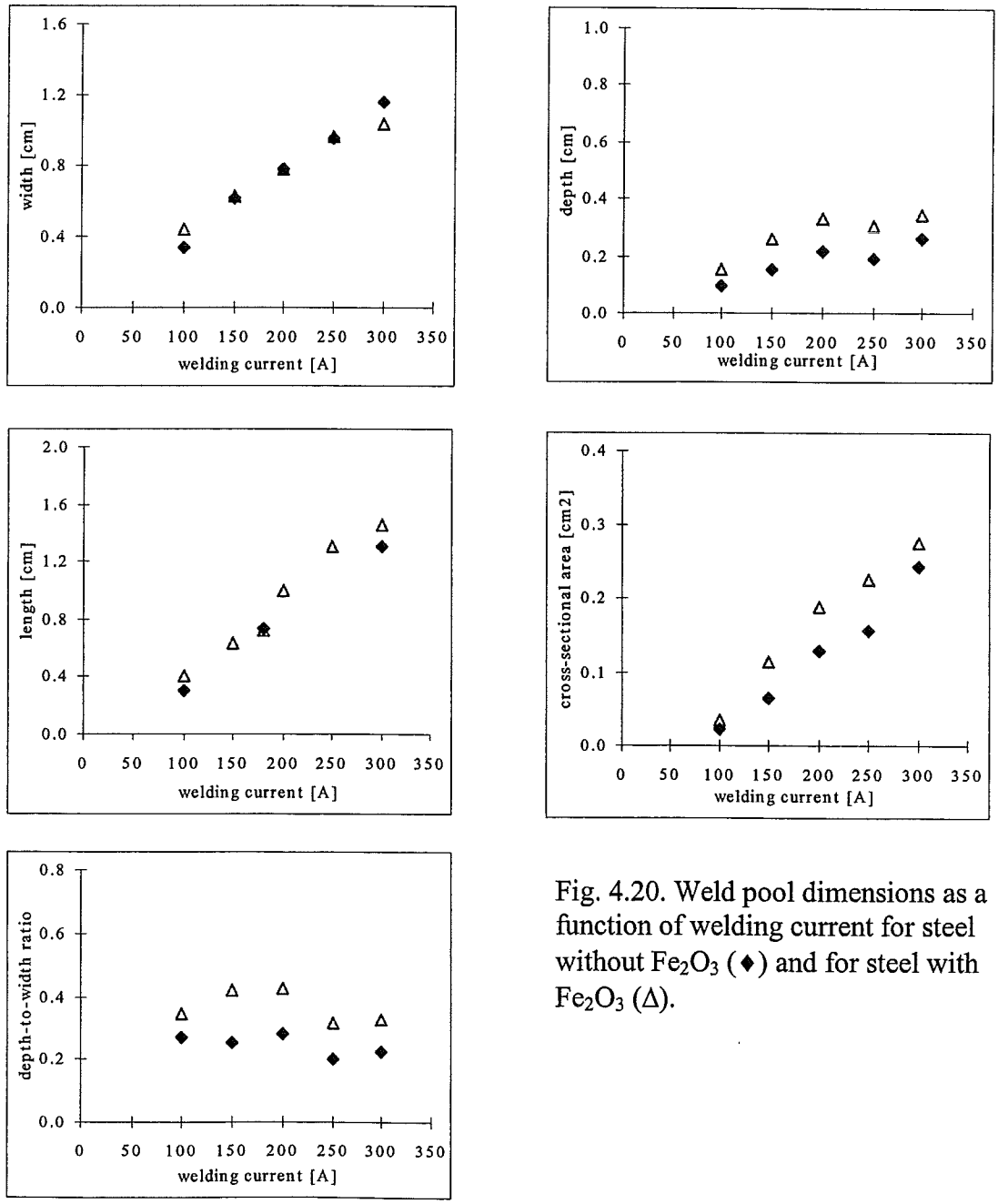

Fig. 4.20. Weld pool dimensions as a function of welding current for steel without Fe_2O_3 (♦) and for steel with Fe_2O_3 (Δ).

current and travel speed show the same behaviour as for welds with SiO_2. However, the arc voltage behaviour as function of the arc length is different from the results with SiO_2.

The changes of the voltage between blank steel and steel with Fe_2O_3 as function of the welding current and the travel speed can be explained in terms of the amount of vaporised additive present in the arc, as already mentioned with SiO_2. With increasing welding current the vapour is removed from the arc by the gas vortex, decreasing the constriction of the arc. With increasing travel speed more Fe_2O_3 is vaporised in the arc increasing the arc constriction and thus the arc voltage.

Differences in voltage behaviour with increasing arc length for SiO_2 and Fe_2O_3 can be explained with the absence of arc trailing. In the case of SiO_2 arc trailing is responsible for part of the increase of the voltage difference with blank steel. Since no significant arc trailing occurs with Fe_2O_3 a smaller increase in voltage difference is expected.

4.2.2 Changes in the weld pool

Photographs of transverse cross-sections of a weld on blank steel and a weld with Fe_2O_3 are shown in Fig. 4.19. Both welds were made under standard welding conditions. The cross-sections show that the width of the weld pool does not change significantly, while the depth strongly increases when Fe_2O_3 is added.

Impact of welding current

Variations in width, depth, depth-to-width ratio, length and cross-sectional area for welds on blank steel and with Fe_2O_3 are shown in Fig. 4.20 as a function of the welding current. Width and length of welds with Fe_2O_3 do not differ much from welds on blank steel. This is different from the results found with SiO_2, where the width is smaller compared to the blank for high currents and the length is longer. The depth of the weld pool for Fe_2O_3 increases more compared to the blank than with SiO_2. Consequently, the D/W ratio and the cross-sectional area also increase when Fe_2O_3 is added, but to a smaller extend than with SiO_2.

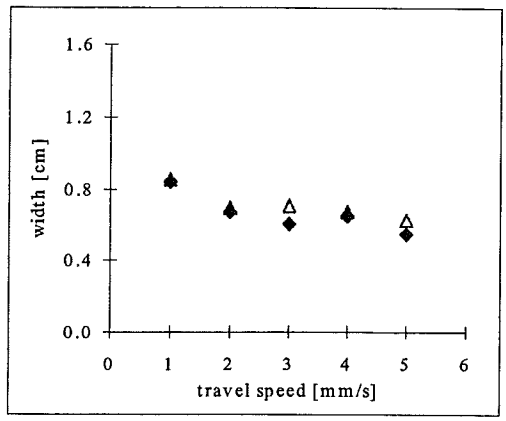

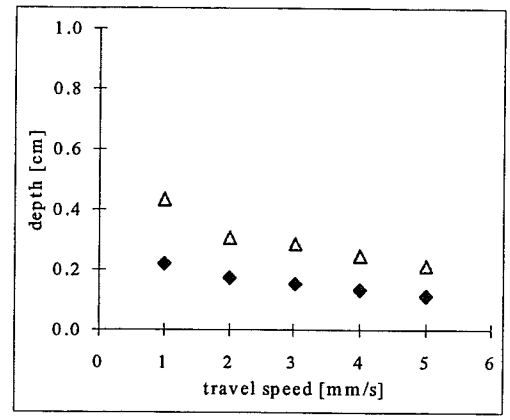

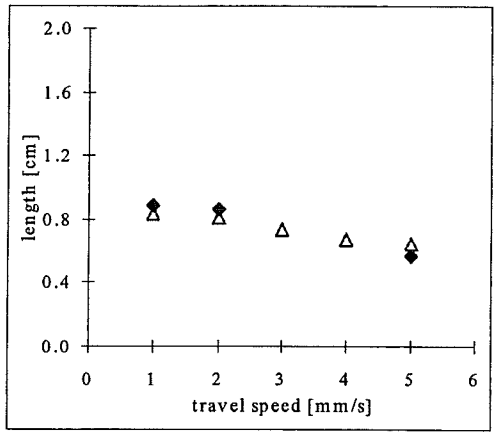

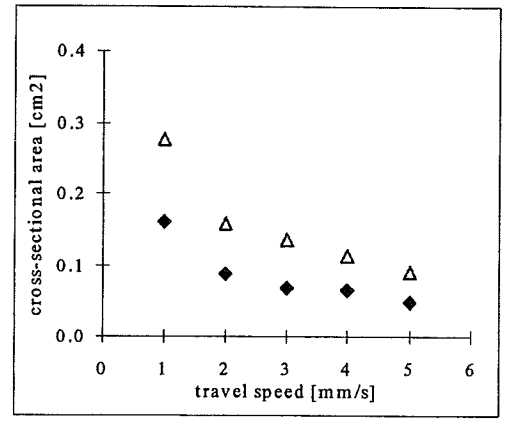

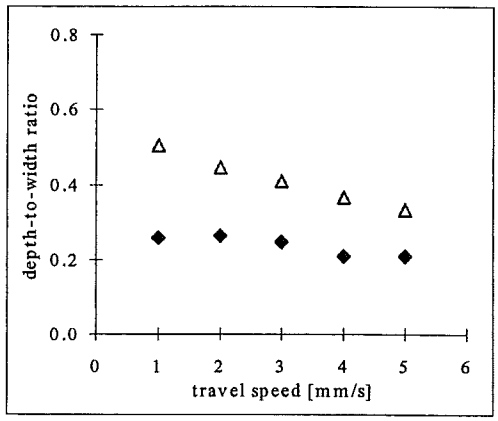

Fig. 4.21. Weld pool dimensions as a function of travel speed for steel without Fe_2O_3 (♦) and for steel with Fe_2O_3 (Δ).

Influence of travel speed

Variations in width, depth, depth-to-width ratio, length and cross-sectional area of the weld pool as a function of the travel speed are shown in Fig. 4.21. No changes occur in width and length compared to the results for blank steel. However, larger depth, D/W ratio and cross-sectional area were observed.

Influence of arc length

Variations of width, depth, D/W ratio, length and cross-sectional area with changing arc length for welds on blank steel and with Fe_2O_3 are shown in Fig. 4.22. It appears that width and length do not change when Fe_2O_3 is added compared to the results for blank steel, while depth and cross-sectional area show a constant increase. The D/W ratio is larger for welds with Fe_2O_3 than for welds on blank steel, but the difference between both curves decrease with increasing arc length.

Discussion of results

The results of width and length measurements of the weld pool between welds with and without Fe_2O_3 for different welding parameters show no significant variations. This is different from the results obtained when SiO_2 is used as additive. In section 4.1 it was argued that SiO_2 at the surface is responsible for the arc trailing as well as for the changes in the arc root. This causes a narrow and elongated weld pools. With Fe_2O_3 on the surface no visible arc trailing occurs and the arc root is not significantly altered. Therefore the layer is expected to have no influence on the width and length of the weld pool.

In contrast with the weld pool width and length, the depth and cross sectional area increase when Fe_2O_3 is added. The increase is equal or even larger than found with SiO_2. However, this can not be induced by a high arc voltage or a changed arc root as was considered for SiO_2. With Fe_2O_3 the increase in depth seems to be a result of changes in the surface tension of the weld pool. The changes D/W observed in the case of Fe_2O_3 are consistent with the results obtained by Burgardt and Heiple [18], shown in Fig. 2.15. These D/W ratios are considered to be a result of a Marangoni flow directed weld pool formation.

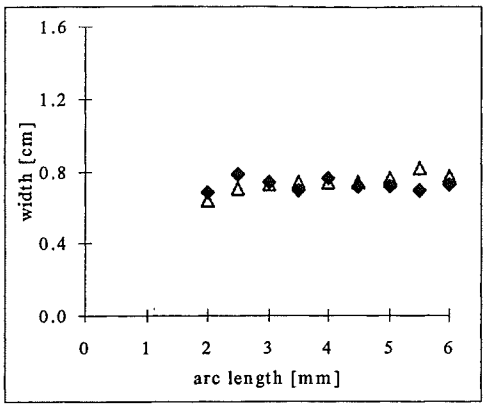

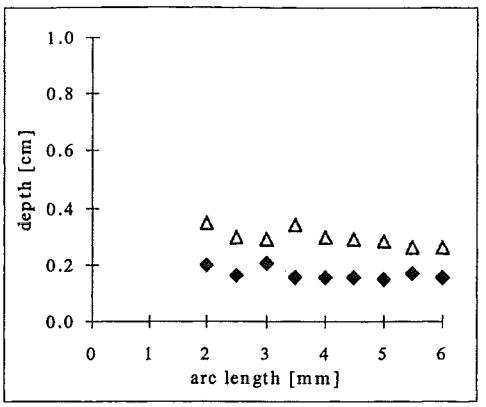

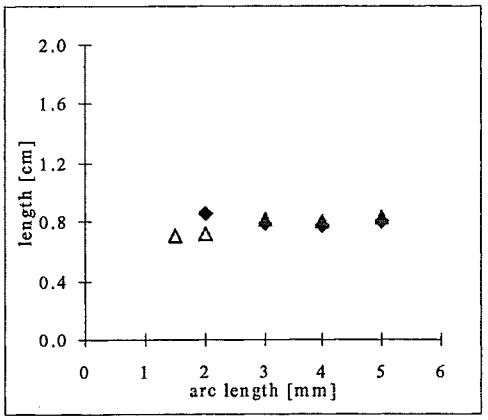

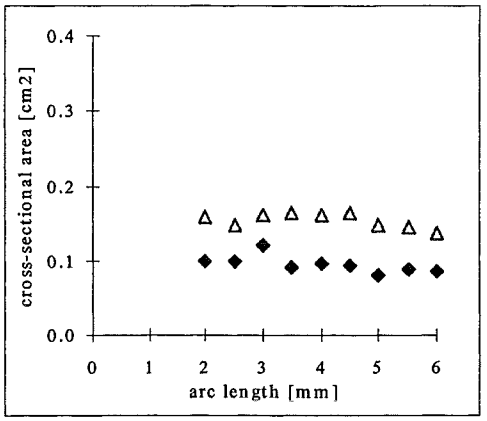

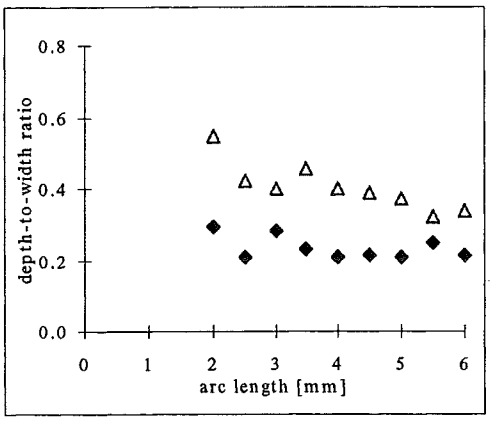

Fig. 4.22. Weld pool dimensions as a function of arc length for steel without Fe_2O_3 (♦) and for steel with Fe_2O_3 (Δ).

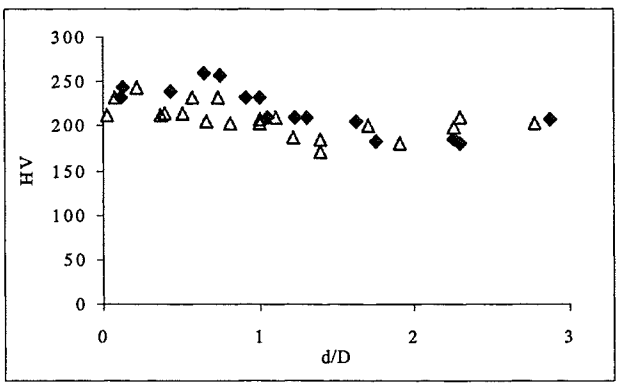

Fig. 4.23. Hardness measurements plotted against the relative depth for steel without Fe_2O_3 (♦) and for steel with Fe_2O_3 (Δ).

With increasing current the depth first increases until 200 A then it decreases again. This is a result of the surface-active elements that loose their influence on the surface tension at high temperature. The D/W ratio with Fe_2O_3 strongly decreases with increasing travel speed. With increasing travel speed the temperature gradient in the weld pool decreases, which results in a weaker Marangony flow. In situations where the weld pool contains a positive surface tension temperature gradient, as is expected with Fe_2O_3, it decreases the inward flow in the weld pool, explaining the large decrease in D/W ratio. With the arc length the D/W ratio also strongly decreases for a weld with Fe_2O_3. With increasing arc length the temperature gradient on the weld pool surface decreases resulting in the same effect as with increasing travel speed.

Apparently, the Marangoni flow has a larger influence on the weld pool with Fe_2O_3 than with SiO_2. With SiO_2 the oxide layer and arc constriction have a dominant effect on the flow in the weld pool and thus on the weld pool dimensions. Also the presence of manganese silicates can play a role.

4.2.3 Hardness, structure and composition of the weld

The results of hardness measurements are shown in Fig. 4.23. The measurements were performed in the same way as with SiO_2. It appears that the weld is slightly affected by the presence of Fe_2O_3. The hardness of the weld metal with Fe_2O_3 is smaller than for blank steel. However, compared to the weld metal with SiO_2 a higher hardness is found. This can be qualitatively explained by taking the effect of Fe_2O_3 on the arc root into account. Fe_2O_3 has much less influence on the shape of the arc root than SiO_2 and no elongated weld pool is formed. Consequently, the weld metal experiences a shorter temperature influence.

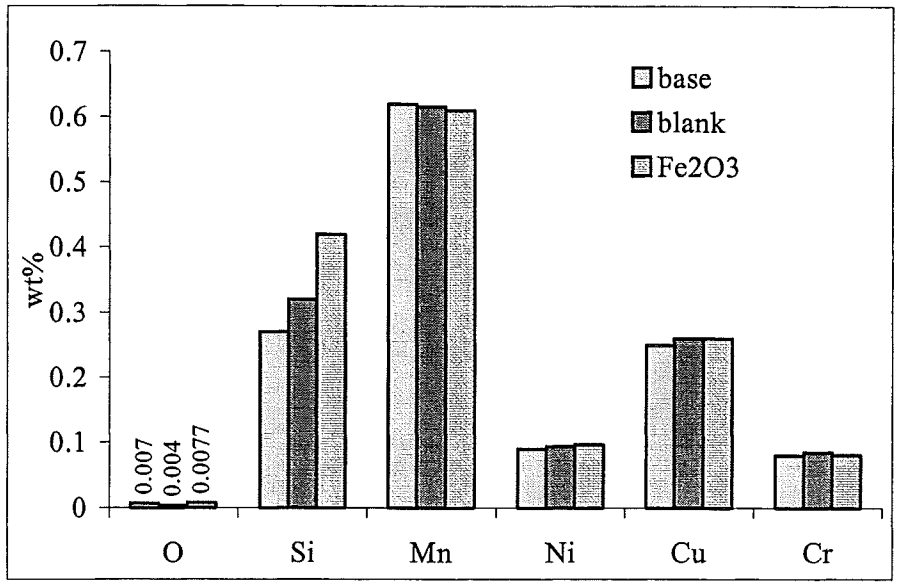

Fig. 4.24. Composition of the base material, weld metal and weld metal with Fe_2O_3.

Composition changes due to Fe_2O_3 addition are shown in Fig. 4.24. Surprisingly, the observed increase in Si wt% is about equal to the increase found when SiO_2 was added. This supports the assumption that most of the Si increase is due to diffusion from the base metal. Typical is the unchanged Mn concentration. When welding with SiO_2 as additive the Mn concentration decreased, with Fe_2O_3 this was not found. This supports the assumption that manganese silicates are formed when SiO_2 is used as additive.

The oxygen concentration does not give any indication of a higher concentration that could influence the surface tension. As already noted before the oxygen concentration should be interpreted under some considerations. For a better indication of the influences of Fe_2O_3 on the surface tension the oscillation frequency of the weld pool should be measured.

Photographs of structure analysis are shown in Fig. 4.25. They were taken of regions that can be compared with those of welds obtained with SiO_2, shown in Fig. 10. The same type of structure is formed although ferrite plates and needles are not as coarse as those found for welds with SiO_2. The structure more or less lies between those formed in blank steel and those formed in steels with SiO_2. This is in agreement with the hardness measurements, shown in Fig. 4.23.

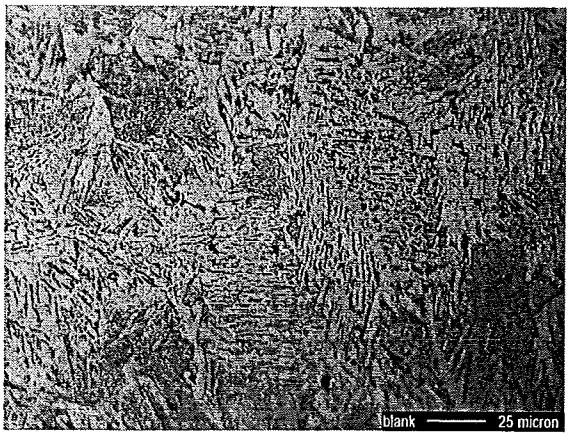

a

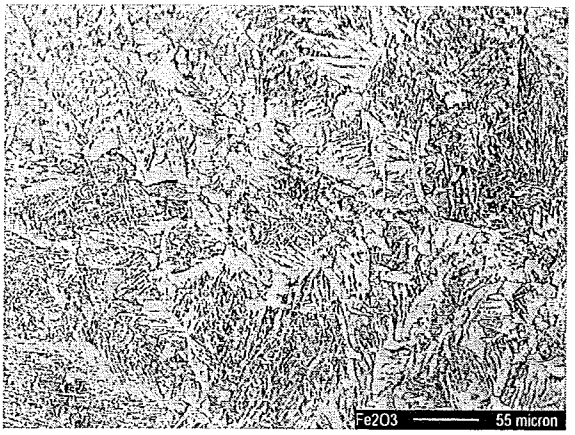

b

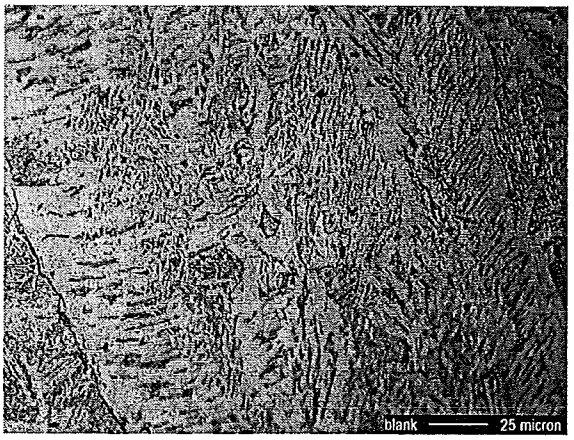

c

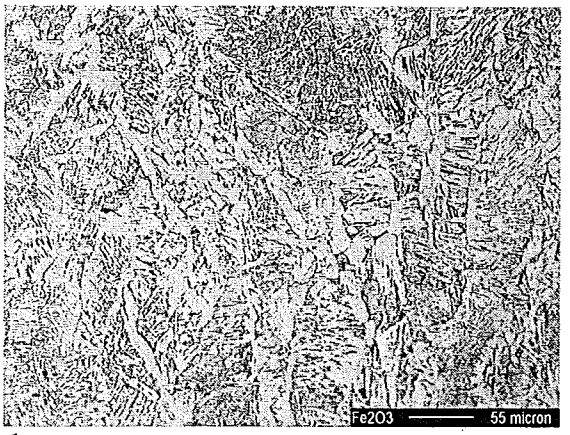

d

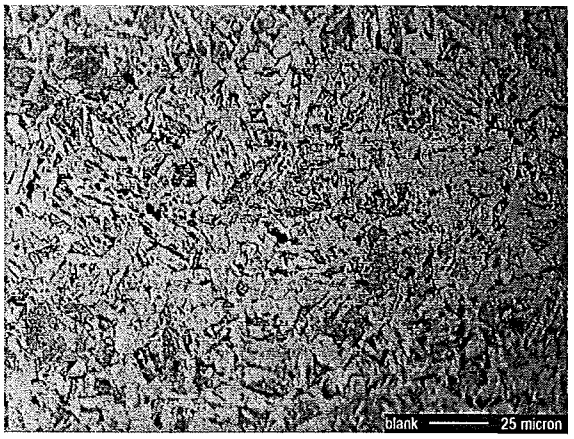

e

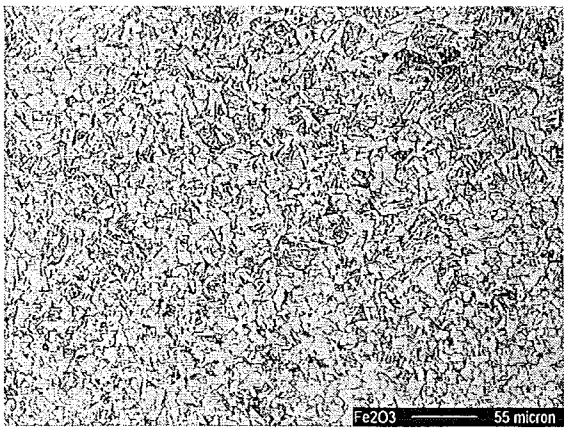

f

Fig. 4.25. Structures of the weld metal (a,c,e for blank steel, b,d,f for steel with Fe_2O_3).
a and b. fusion zone
c and d. fusion boundary
e and f. HAZ

5. Conclusions and recommendations

The experimental results described in this report indicate that changes in the arc and weld pool caused by additives can be considered to be mainly caused by three mechanisms: arc constriction, arc root deformation and changes in Marangoni flow.

Arc constriction is observed during the welding process with additive. Voltage measurements show a considerable increase when the arc is constricted. The diminished arc constriction at higher welding current indicates the importance of the amount of vaporised additives in the arc. Also tests with increased layer thickness of SiO_2 confirm this conclusion.

Changes in the arc root configuration are primarily noticed during the observation of the welding arc, in the form of arc trailing. Other effects on the arc root are found when the weld metal is blown out of the weld pool. Welds with SiO_2 added show a strongly elongated weld pool with a smaller width. Width and length of welds made with Fe_2O_3 show smaller changes in comparison with those of blank steel than SiO_2, which is similar to the smaller effect on arc trailing. The differences between the results for SiO_2 and Fe_2O_3 emphasise the importance of the physical properties of the additives.

The Marangoni flow is thought to cause depth variations and changes in the D/W ratio with Fe_2O_3 at high current. It seems that with Fe_2O_3 the Marangoni flow is not suppressed by the presence of the oxide layer, as is probably the case with SiO_2. Chemical analyses of the welds with Fe_2O_3 show no increase in concentration of oxygen. However, the oxygen is present at the surface of the weld and could have been removed during the preparation of the sample for chemical analysis.

A direct indication of the influences of additives on the surface tension was obtained by determining the surface tension with a weld pool oscillation technique. In this research project, the results give only an indication of the variation of the surface tension of the weld pool with the temperature. A large difference in surface tension exists between welds on blank steel and with SiO_2. However, for both welds a negative surface tension

temperature coefficient is found. This is probably caused by the high temperature of the weld pool.

Hardness measurements indicate that the oxide layer slightly changes the mechanical properties of the weld. This is in agreement with the different structures of the welds.

Further understanding of the mechanisms that play a role in weld pool formation can be obtained by additional experiments. High-speed filming of the arc will provide more information of the interaction of the arc with the oxide layer. The vapours that are present in the arc could be determined with spectroscopic analyses.

The set–up for weld pool oscillation measurements should be improved in order to make it possible to determine the surface tension at lower temperatures on an abstract scale. Oscillation measurements of molten steel in a cup instead of on a plate should be considered. The heating can then be induced by an induction heater, providing a weld pool almost without a temperature gradient. Another advantage is that the welding current can be kept constant and does not have to increase in order to increase the temperature of the molten metal. Surface tension measurements were performed with SiO_2 and these experiments still have to be carried out with Fe_2O_3.

So far, hardness measurement did not show an important alteration of the weld properties. Composition and structure analyses gave the impression that the oxide forms no inclusions in the weld metal. However, more research should be carried out to changes in the mechanical properties of the weld

Finally, it can be stated that SiO_2 and Fe_2O_3 can be well used as tracers. The arc voltage alters with both oxides, which makes the use as tracer possible. They both improve the penetration properties of the weld. Hardness measurements and structure analysis have shown no negative effects until now, but additional research should be carried out.

References

[1] W. Middel and G. Den Ouden
The effect of additives on arc characteristics in GTA welding.
1998

[2] G. Den Ouden
Lastechnologie.
ISBN 90-6562-087-7
Delftse Uitgevers Maatschappij B.V. Third edition, 1993

[3] J. Zijp
Heat transport during Gas Tungsten Arc Welding.
PhD-thesis, Welding Department
Faculty of Materials Science and Engineering, Technical University of Delft
February 1996

[4] T. W. Eagar and N, -S. Tsai
Temperature fields produced by traveling distributed heat sources.
Welding Journal, Vol. 62 (12), pp. 346s-355s
December 1983

[5] N. Christensen, V. de L. Davies and K. Gjermundsen
Distribution of temperatures in arc Welding.
British Welding Journal, Vol. 12, pp. 54-65
March 1964

[6] N. S. Tsai and T. W. Eagar
Distribution of the heat and current fluxes in gas tungsten arcs.
Metallurgical Transactions B, Vol. 16B, pp. 841-845
December 1985

[7] H. A. Dinulescu and E. Pfender
Analysis of the anode boundary layer of high intensity arcs.
Journal of applied physics, Vol. 51 (6), pp. 3149-3157
June 1980

[8] Yu V. Kazakov
Effect of activating fluxes on the structure of the welding arc in argon.
Svar. Proiz., (4), pp. 30-32
1985

[9] W. H. Giedt, L. N. Tallerico and P. W. Fuerschbach
GTA welding efficiency: Calorimetric and temperature field measurements.
Welding Journal, Vol. 68 (1), pp. 29s-32s
January 1989

[10] T. Aendenroomer
Weld pool oscillation for penetration sensing and control.
PhD-thesis, Welding Department
Faculty of Materials Science and Engineering, Technical University of Delft
September 1990

[11] M. M. Savitskii and G. I. Leskov
The mechanism of the effect of electrically negative elements on the penetration power of an arc with tungsten electrode.
Automatic Welding, Vol. 33 (9), pp. 11-16
September 1980

[12] W. Lucas, D. Howse, M. M. Savitsky and I. V. Kovalenko
Activated flux increasing the performance and productivity of the TIG and plasma processes.
TWI, Cambridge, UK & Paton Welding Institute, Ukraine
IIW Doc. XII-1448-96
1996

[13] H. C. Ludwig
Current density and anode spot size in the gas tungsten arc.
Welding Journal, Vol. 47 (5), pp. 234s-240s
May 1968

[14] Yu V. Kazakov, K. B. Koryagin and V. P. Potekin
Effect of activating fluxes on penetration in welding steel thicker than 8 mm.
Welding International, Vol. 5 (3), pp. 202-205
May 1991

[15] Sindo Kou and D. K. Sun
Fluid flow and weld penetration in stationary arc welds.
Metallurgical Transactions A, Vol. 16A, pp. 204-213
February 1985

[16] Akira Matsunawa, Shinichiro Yokoya and Yutaka Asako
Convection in weld pool and its effect on penetration shape in stationary arc welds.
Transactions of JWRI, Vol. 16, pp. 229-236
February 1987

[17] K. Hong, D. C. Weckman and A. B. Strong
The predicted influence of turbulence in stationary gas tungsten arc welds.
Trends in Welding Research
June 1995

[18] P. Burgardt and C. R. Heiple
Interaction between impurities and welding variables in determining GTA weld shape.
Welding Journal, Vol. 65, pp. 150s-155s
June 1986

[19] R. A. Woods and D. R. Milner
Motions in the weld pool in arc welding.
Welding Journal, Vol. (50), pp. 163s-173s
April 1971

[20] K. C. Mills and B. J. Keene
Factors affecting variable weld penetration.
International Materials Reviews, Vol. 35 (4), pp. 185-125
April 1990

[21] B.J. Keene, K.C. Mills, J.W. Bryant and E.D. Hondros
Effect of interaction between surface active elements on the surface tension of iron.
Canadian Metallurgy Quarterly, Vol. 21 (4), pp. 393-403
1982

[22] C. R. Heiple and J. R. Roper
Mechanism for minor element effect on GTA Fusion zone geometry.
Welding Journal, Vol. 61 (4), pp. 97s-102s
April 1982

[23] A. A. Shirali and K. C. Mills
The effect of welding parameters on penetration in GTA welding.
Welding Journal, Vol. 72, pp. 347s-353s
July 1993

[24] J. Franse, T. Luyendijk and G. den Ouden
Vorm en grootte van het lasbad.
Lastechniek, Vol. 50 (5), pp. 82-87
May 1984

[25] Welding handbook.
ISBN 0-87171-126-5
American Welding Society
Seventh edition, 1976

[26] Internet
http://home.istar.ca/~bsant/WeldMet/CMn.html
The welding engineer's weld pool.
The Welding Institute (TWI), Abington, UK

[27] C. R. Heiple, J. R. Roper, R. T. Stagner and R. J. Aden
Surface active element effects on the shape of GTA, laser and electron beam welds.
Welding Journal, Vol. 62 (3), pp. 72s-77s
March 1983

[28] B. Pollard
The effect of minor elements on the welding characteristics of stainless steel.
Welding Journal, Vol. 67 (9), pp. 202s-213s
September 1988

[29] A. A. Sherali
Effect of trace elements on penetration of TIG/GTA welds.
Joining Science, Vol. 1 (3), pp. 167-174
March 1992

[30] P. Sahoo, T. Debroy and M. J. McNallan
Surface tension of binary metal - Surface active solute system under conditions relevant to welding metallurgy.
Metallurgical Transactions B, Vol. 19B, pp. 483-491
June 1988

[31] W. Lucas and D. Howse
Activating flux increasing the performance and productivity of the TIG and plasma
processes.
Welding and Metal Fabrication, pp. 11-17
January 1996

[32] You Hong Xiao
Weld pool oscillation during gas tungsten arc welding.
PhD-thesis, Welding Department
Faculty of Materials Science and Engineering, Technical University of Delft
April 1992

[33] Y. H. Xiao and G. den Ouden
Measurement of surface tension of liquid metal and alloys under arc welding conditions.
Materials Science and Technology, Vol. 13, pp. 791-794
September 1997

[34] S. E. Offerman
Theoretical and experimental development of surface tension measurements under arc plasma conditions.
Master thesis
Faculty of Materials Science and Engineering, Technical University of Delft
April 1999

[35] ASTM Standard E92-72